

Energy and Electron Transfer in Photochromic Molecules

by

Jeffrey Crisman

A Dissertation Presented in Partial Fulfillment
of the Requirements for the Degree
Doctor of Philosophy

Approved April 2014 by the
Graduate Supervisory Committee:

John Gust, Chair
Seth Rose
Ana Moore

ARIZONA STATE UNIVERSITY

May 2014

ABSTRACT

Photochromic molecules, which photoisomerize between two chemically and optically distinct states, are well suited for electron and energy transfer to covalently attached chromophores. This dissertation aims to manipulate electron and energy transfer by photochromic control in a number of organic molecular systems. Herein the synthesis, characterization and function of these organic molecular systems will be described. Electron and energy transfer were quantified by the use of steady state absorbance and fluorescence, as well as time-resolved fluorescence and transient absorbance. A dithienylethene-porphrin-fullerene triad was synthesized to investigate photochromic control of photo-induced electron transfer. Control of two distinct electron transfer pathways was achieved by photochromic switching. A molecular dyad was synthesized, in which fluorescence was modulated by energy transfer by photoinduced isomerization. Also described is a triplet-triplet annihilation upconversion system that covalently attaches fluorophores to improve quantum yield. Overall these studies demonstrate complex molecular switching systems, which may lead to advancement in organic electronic applications and organic based artificial photosynthesis systems.

DEDICATION

I would like to dedicate this dissertation to my loving parents, Pam and Jerry

ACKNOWLEDGMENTS

I am very grateful to so many people for helping me out throughout my graduate studies. First, I would like to thank my advisor Devens Gust for guiding me along this long journey. I would also like to thank Ana and Tom Moore and the rest of the Gust/Moore/Moore group for providing me with a laboratory and funding. Special thanks to Stephen Straight, Julien Frey, Yuichi Terazono, Graeme Copley, and Jason Gillmore and Paul Liddell for synthetic advice. I would like to give a big thank you to Michael Hambourger for showing me how to transition into graduate school, and for all his generously donating his time to help me out with any project I was working on no matter how laborious. I would like to extend a big thank you to Gerdenis Kodis for running all the photochemistry experiments, even when it became repetitive and seemed like the experiment was going nowhere.

A very special thanks goes to Michael J. Shaw, for allowing me to work in his lab as an undergraduate. You showed me how to work with air sensitive chemicals, and the basic synthetic skills I needed for graduate school.

I must thank Chris Madden, Jesse Bergkamp, Ben Sherman, Dustin Patterson, Michael and Natalie Vaughn, Manuel Portolés, and Jim Bridgewater for being great friends and enduring Fuj, when he came out to play. You all are life long friends and I hope we can collaborate and share some more of life's pleasures. Your continued advice has helped transform me into the person I am today, for which I am extremely grateful.

Jody Mitchell and Tim Wolfrum, you two have been great neighbors and have shown me the true meaning of friendship. No matter what obstacle was in my way your advice was always well received. I would also like to thank you for purchasing the sport packages and providing me with a place to watch sports.

Finally I would like to thank my parents. Mom, you showed me at an early age what education means, and I would not be here without you. Both of your support over the years has gotten me through a lot whether it was the best or worst of times. I love you.

TABLE OF CONTENTS

	Page
LIST OF FIGURES	v
CHAPTER	
1 INTRODUCTION	1
2 PHOTO-INDUCED ELECTRON TRANSFER IN A TRIAD	5
Molecular Design	5
Synthesis.....	6
Photochemistry	6
Energetics	14
Conclusion	15
3 PHOTOCROMIC MODULATION OF FLUORESCENCE	17
Molecular Design	17
Synthesis.....	18
Photochemistry	18
Modulation of Fluorescence	20
Energetics	22
Concusion	23
4 A TRIPLET-TRIPLET ANNIHILATION UPCONVERSION SYSTEM	24
Introduction	24
Synthesis.....	26
Photochemistry	27
Conclusion	28
5 EXPERIMENTAL PROCEDURES	29
Experimental Procedures	29
General Instrumentation Techniques.....	29
Experimental for Chapter 2	31
Experimental for Chapter 3	35

Experimental for Chapter 4	42
REFERENCES.....	44

LIST OF FIGURES

Figure		Page
1.	Structure of DTE Model, Dyad 2, and Triad 1	7
2.	Time Resolved Fluorescence and UV-vis absorption of DTE	8
3.	UV-vis Absorption and Emission Scans of Dyad 2	9
4.	Time Resolved Fluorescence of Dyad 2	10
5.	Transient Absorption Kinetic plot of Dyad 2	11
6.	UV-vis Absorption and Emission Scans of Triad 1	12
7.	Time Resolved Fluorescence of Triad 1	13
8.	Transient Absorbance of Triad 1	14
9.	Energy Level Diagram of Triad 1	15
10.	UV-vis Absorption of 20	18
11.	UV-vis Absorption of Model BPEA, 18, and 20	19
12.	Square Wave Modulation of Fluorescence	21
13.	Sine Wave Modulation of Fluorescence	22
14.	Structure of Hexad 21 and Monomer 22	26
15.	Absorbance Spectra of Monomer, Hexad, and Porphyrin	27
16.	Emission Spectra of TTA-UC	28
17.	Synthetic Scheme of Dyad 3	34
18.	Synthetic Scheme of Triad 1	35
19.	Synthetic Scheme of 19	40
20.	Photoisomerization of Model Photochrome	40
21.	Synthetic Scheme of 18	41
22.	Synthetic Intermediates and Final Compounds for TTA-UC	43

CHAPTER 1

INTRODUCTION

This dissertation will describe the synthesis and characterization of covalently attached organic chromophores to photochromic molecules. Spectroscopic studies on these molecules show that these molecules can manipulate photochemical and photophysical processes, which can lead to a wide variety of potential uses.

Photochemistry is the study of absorption of light by molecules. An example of photochemistry is the process of photosynthesis. Absorption of light allows plants to convert carbon dioxide into sugar, without this process life on earth would cease to exist. In order for a molecule to absorb light, its highest occupied molecular orbital (HOMO) and lowest unoccupied molecular orbital (LUMO) energy gap must match the energy of the incident photon. The photon's energy is absorbed, allowing an electron to be promoted from the highest occupied molecular orbital (HOMO) to the lowest unoccupied molecular orbital (LUMO), generating an excited state of the molecule. Once this energy is absorbed, a variety of process can occur.

Most molecules, with a few exceptions, in the ground state have paired electrons; this is called a singlet state. When a molecule absorbs light, the excited electron is still paired to the ground state electron, creating a singlet excited state. A triplet state is the result of an unpaired excited electron. Direct conversion of a ground state electron to the triplet state is forbidden. The properties of molecule in a singlet state differ greatly from the triplet state, for instance a triplet state molecule is paramagnetic, while the single state is diamagnetic. From the singlet state a variety of processes can occur that returns the molecule to the electronic ground state. Processes relevant to this dissertation are fluorescence, electron transfer, energy transfer, photoisomerization, and intersystem crossing to the triplet state.

One process that can occur is fluorescence. The most useful fluorescence occurs from the $\pi \rightarrow \pi^*$ transition because the energy required brings the absorption peaks into a experimentally convenient spectral region. In order for fluorescence to occur, the molecule usually returns to its lowest excited state by a series of vibrational relaxations releasing heat. From the lowest excited

state the molecule returns to the electronic ground state by emitting a photon, which is in lower in energy than the photon absorbed. This causes the emission to be red shifted, the Stokes shift, from the absorbed photon. Fluorescence can also be greatly influenced by solvent and temperature. An increase in temperature or decrease in solvent viscosity increases the likelihood of deactivation by external conversion or energy transfer to solvent or solutes present. Incorporation of heavy atoms in the solvent reduces fluorescence by increasing the rate of triplet formation, thus increasing the phosphorescence of the molecule. Dissolved oxygen often reduces fluorescence intensity, by intersystem crossing and conversion of the singlet state to the triplet state. However this effect may be caused by photochemically induced oxidation of a fluorescing molecule.¹

Photoinduced electron transfer can occur when an easily reduced or oxidized molecule is excited and is in close proximity to another molecule of appropriate redox potentials. The rate of electron transfer can be determined from the classic Marcus equation,^{2,3}

$$k_{ET} = \sqrt{\pi / \hbar^2 \lambda k_b T} |V|^2 e^{-\frac{(\Delta G^\circ + \lambda)^2}{4\lambda k_b T}} \quad (1)$$

where ΔG° , the driving force of the reaction, is the standard free energy of reaction, \hbar is Planck's constant divided by 2π , k_b is Boltzmann's constant, T is the absolute temperature, and V is the matrix element. The maximum rate of electron transfer k_{ET} happens when $-\Delta G^\circ = \lambda$, the reorganization energy.

Energy transfer occurs when an excited state molecule, the energy donor, donates its energy to another molecule, the energy acceptor. This process can be thought of as the energy donor emitting a photon, and being absorbed by the energy acceptor, although this process does not actually occur. Thus, energy transfer is possible if the emission of the energy donor overlaps with the absorption of the energy acceptor. If the molecules are covalently linked, and are far enough apart that their orbitals do not overlap, energy transfer is given by the Förster equation^{4,5}

$$k_{EFT} = \frac{0.04\pi^2 \kappa^2 \phi_D}{n^4 N_A^2 R^6} J \quad (2)$$

where κ is an orientation factor, Φ_D is the quantum yield of the fluorescence donor, n is the dielectric constant of the medium, N is Avogadro's number, τ_D is the excited state lifetime of the donor in absence of energy transfer, R is the distance between chromophores, and J is a function of the spectral overlap of the donor's emission and the acceptor's absorption. For the work presented here energy transfer will be thought of as by Förster mechanism.

Photoisomerization occurs when absorbed energy is dissipated by breaking and forming covalent bonds to create two chemically and optically distinct states. Photochromic molecules are a class of organic molecules where isomerization is photochemically and often times thermally reversible. The work in this dissertation can be divided into two classes of photochromic molecules. The first class of molecules undergoes a $6e^-$ electrocyclization where a sigma bond is either broken or formed. Typically these molecules are synthesized in their open form, which absorbs in the UV region of the electromagnetic spectrum. UV absorption leads to closing of the ring which shows a new absorption in the visible region as well as different redox properties. Irradiation of the closed form, results in isomerization back to the open form. These molecules are typically thermally stable in both isomeric forms.^{6,7} Diarylethenes are a type of these photochromes and will be utilized in this work.

The second class of photochromic molecules used in this work is a spiro type photochrome. Bond breakage occurs at a spiro-type carbon, opening either a 5 or 6 membered ring, resulting in a zwitterionic open form. Ring opening occurs when UV light is absorbed, however ring closure is usually thermal.^{7,8} Typically, these molecules in their ground state are in the closed colorless form. However, the photochrome, used in this work is in its zwitterionic open form in its electronic ground state. These photochromes, where the ground state isomer is reversed, are called reverse photochromes.

Triplet-triplet annihilation up conversion (TTA-UC) is a process in which lower energy photons can be converted to higher energy photons.^{9,10} This process occurs in three steps. The first step excites a triplet sensitizer quickly yielding a triplet excited state.^{11,12} This energy is then transferred to a fluorophore to give an emitter triplet state. The final step requires one triplet

emitter to donate its energy to another triplet emitter, resulting in a single singlet excited state, which then emits by normal fluorescence pathways. This process requires two diffusion steps, one to generate the emitter triplet state, and one to generate the singlet excited state. In order to improve TTA-UC this work seeks to reduce the number of diffusion steps by covalently attaching the emitters.

In Chapter 2, photo-induced electron transfer from the porphyrin moiety to the fullerene moiety, in a dithienylethene(DTE)-porphyrin(P)-fullerene(C₆₀) triad, occurs until the dithienylethene moiety is photoisomerized to its closed form. This leads to electron transfer from the DTE unit to the porphyrin, where charge recombination is extremely quick. The original approach of this work was to create a long lived charge separated state between the DTE unit and fullerene.

In Chapter 3, fluorescence is modulated in a spiroxazine(SO)-bis(phenylethynyl)anthracene(BPEA) dyad. Excitation of BPEA allows strong emission when the spiroxazine moiety is in its closed form (SO_c), however fluorescence is strongly quenching when the spiroxazine moiety is in the open form (SO_o) by singlet-singlet energy transfer. This energy transfer causes isomerization of SO_o to SO_c allowing for stronger BPEA emission. Photoisomerization of SO_o to SO_c increases BPEA fluorescence as well. Fluorescence quenching is returned when spiroxazine thermally isomerizes back to the closed form.

In Chapter 4, red light was upconverted to green light. One possible application of many would be to increase efficiency of various solar cells by utilizing TTA-UC.¹³ The system made involved attaching BPEA fluorophores to a hexaphenyl benzene core. This covalent attachment of fluorophores reduces the number of diffusion steps, which improves the upconversion process.

In Chapter 5, synthetic and characterization of molecules described herein are given. Experimental apparatuses used to study synthesized molecules are also described.

CHAPTER 2

PHOTO-INDUCED ELECTRON TRANSFER IN A TRIAD

Molecular Design. Photochromic molecules are classified as reversible dyes under photochemical control, in which absorbed electromagnetic radiation isomerizes the molecule between two states with different absorption and redox properties. Thermally stable photochromic molecules have shown to be good candidates for light controlled molecule-based devices.¹⁴⁻¹⁷

Liddell *et al.* reported a dithienylperfluorocyclopentene (DTEF)-porphyrin (P)-fullerene (C_{60}) triad in which photoinduced electron transfer between C_{60} and porphyrin moieties could be controlled by photonic switching of the DTEF moiety.¹⁸ With the DTEF switch in the colorless, open form, excitation of the porphyrin chromophore leads to a photo-induced electron transfer to the C_{60} acceptor. Photoinduced electron transfer between the porphyrin and C_{60} was shown to be controlled by very fast singlet energy transfer from the porphyrin excited state to the colored, closed state of the DTEF switch.

In addition, Effenberger and co-workers reported an anthracene (A)-dithienylethenepyridinium (DTEP) dyad in which the anthracene excited singlet state was quenched by electron transfer to DTEP in the open form creating a charge separated state.¹⁹ However, anthracene's excited-singlet state was also quenched when the DTEP moiety was in the closed form. No anthracene radical cation was observed in this form; thus the quenching of excited singlet state was attributed to energy transfer to DTEP.

Dithienylethenes (DTE) are well studied photochromes, generally associated with high fatigue resistance and thermal irreversibility properties that are essential for serviceable optoelectronic devices and various switching applications.⁶ Although dithienylperfluorocyclopentenenes (DTEFs) are the most studied type of diarylethenes²⁰, dithienylperhydrocyclopentenenes (DTEHs), which are similar in structure to DTEFs and show similar light induced isomerization, can be made from inexpensive starting materials and on a large scale,²¹ but they have been shown inferior to DTEFs in fatigue resistance and spectral splitting.^{21,22} Encouraged by these findings as well as

the lower oxidation potential of dithienylperhydrocyclopentenes (DTEHs) in the closed form, we have prepared dithienylperhydrocyclopentene (DTE)- porphyrin (P)- fullerene (C_{60}) triad **1** as an electron transfer switch to achieve a final $DTE_c^+-P-C_{60}^-$ charge separated state.

Synthesis. Figure 18 shows the synthetic pathway taken to achieve **1**. Synthesis began with a Lindsey condensation of mesityl dipyrromethane, methyl 4-formylbenzoate, and 4'-bromo-4-carbaldehyde-biphenyl to give porphyrin **7**. Meanwhile, chlorines on 2,2-(dichlorodithienyl)-cyclopentene **5** are easily converted into asymmetric bis(boronic) esters using 1 equivalent of *n*-BuLi, followed by Suzuki coupling reaction with the appropriate aryl halide to form **6** and dyad **2**. The Prato reaction using *t*-butyl-4-formylphenyl carbamate, and sarcosine, and followed by deprotection of the amide resulted in **8**. Saponification of the methyl ester of dyad **2** followed by dmap coupling of **8** gives **1**.

Photochemistry. The photochemistry of the DTE model and DTE-P dyad **2** will first be described, followed by the results for triad **1**.

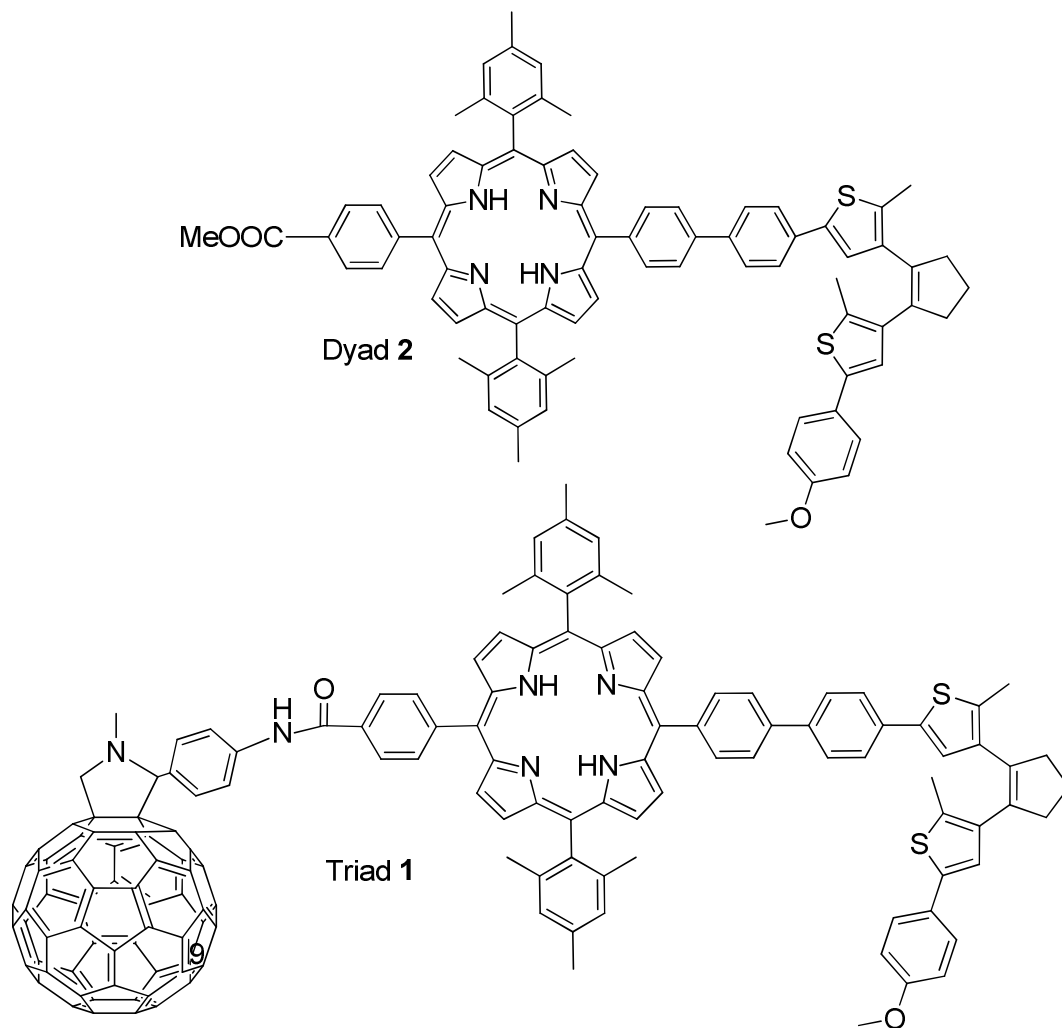


Figure 1. Structure of DTE model, Dyad 2, and Triad 1

Isomerization of DTE₀ to the DTE_c form is accomplished by irradiation with ~312 nm light, with reverse isomerization back to the DTE₀ form by white light, shown in figure 1. The absorption

spectra of DTE_o and DTE_c in 2-methyltetrahydrofuran are shown in Figure 2 inset.

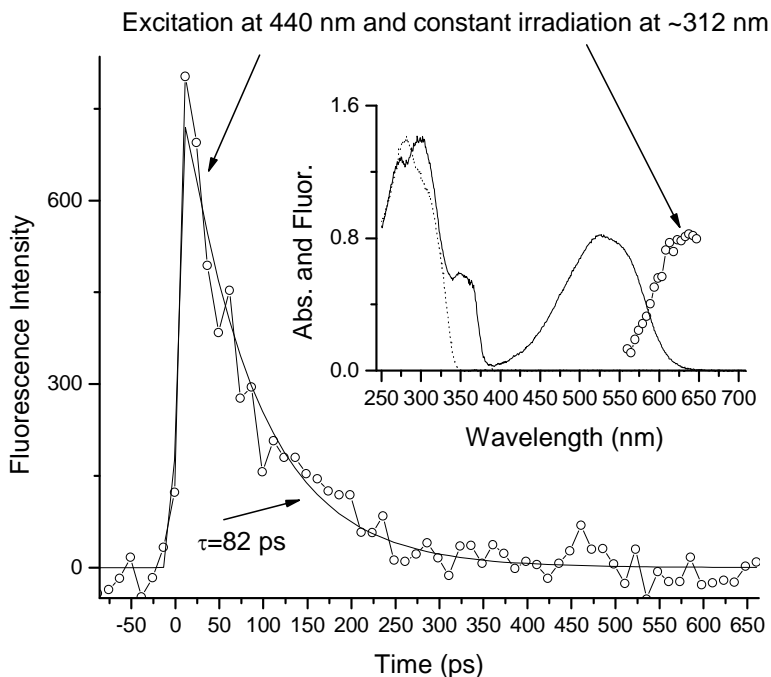


Figure 2. Time Resolved Fluorescence and UV-vis absorption of DTE. **Inset** shows absorbance spectra for DTE_o (dashed) DTE_c black and emission spectra for DTE_c (dotted)

The DTE_o absorption maximum is at 282 nm and DTE_c absorption maxima are at 304 and 530 nm. Time resolved fluorescence shows DTE_c excited state lifetime is 82 ps shown in Figure 2. NMR experiments showed a peak decrease of thiophene aryl hydrogens and a peak increase upfield by about 0.6 ppm. NMR results show about 35% DTE closure in the model, but after 20 minutes of continuous irradiation of light at 312 nm peak increase/decrease stopped.

The absorption spectra of dyad **2** (Figure 3) shows absorption maxima at 419 (Soret), 514, 549, 592, and 646 nm for dyad DTE_o-P and 419 (Soret), 519, 549, and 590 for dyad DTE_c-P.

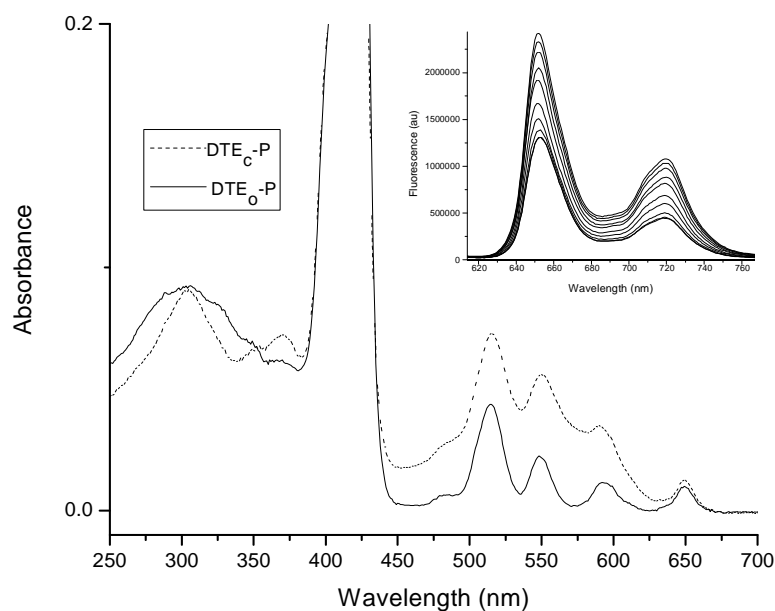


Figure 3: UV-vis Absorption and Emission Scans of Dyad 2

Steady state fluorescence measurements show a decrease in porphyrin fluorescence when DTE is photoisomerized to the closed form, shown in Figure 3 inset. Optical experiments reveal a photostationary state distribution containing approximately 40% DTE_c estimated from DAS and fluorescence measurements. Complete quenching of porphyrin fluorescence is not exhibited and is attributed to low photostationary state distribution.

To further investigate fluorescence quenching, time resolved fluorescence experiments were done in 2-methyltetrahydrofuran. A solution of dyad 2 ($\sim 1 \times 10^{-5} \text{M}$) was excited at 400 nm and emission was measured at 720 nm under constant UV irradiation ($\sim 312 \text{ nm}$) to insure maximum photostationary state distribution of DTE_c-P dyad, shown in Figure 4.

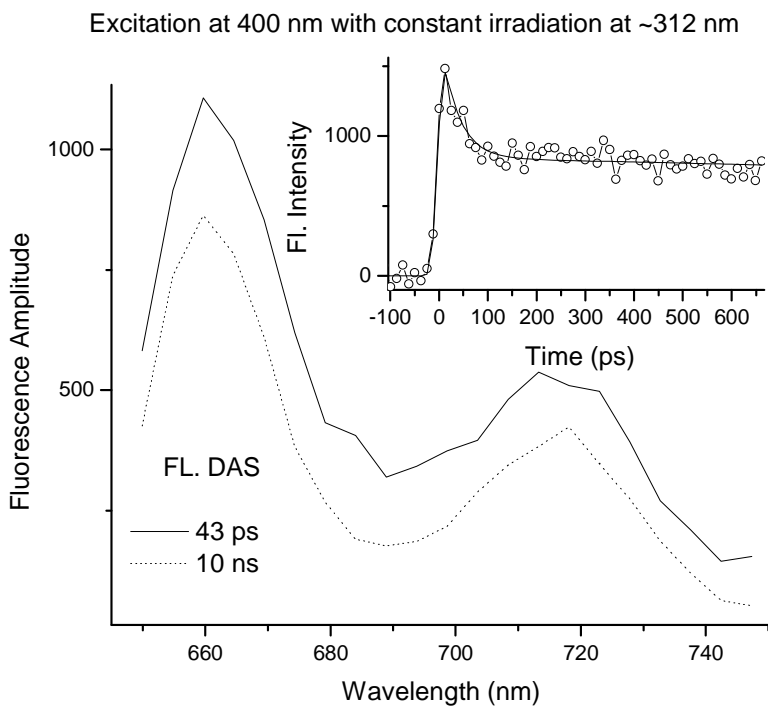


Figure 4. Time Resolved Fluorescence of Dyad 2

The data required two exponentials, with lifetimes of 43 ps and 10 ns. The 10 ns component was ascribed to normal porphyrin decay in dyad $DTE_o\text{-P}$ while the 43 ps component was ascribed to dyad $DTE_c\text{-P}$. Thus, the time resolved fluorescence indicates quenching of the porphyrin first excited state by DTE_c .

The fluorescence quenching in dyad 2 was also examined by using transient absorbance spectroscopy using 100 fs laser pulses at 650 nm under constant UV irradiation (~312 nm). Figure 5 shows the transient absorption spectrum at 700nm showing three exponential components, with time constants of 1.1 ps, 42.8 ps, and 10 ns. The rising 1.1 ps is ascribed to the decay of $DTE_c^+\text{-P}^-$, while the 42.8 ps decay was attributed to the formation of $DTE_c^+\text{-P}^-$. The 10ns decay was ascribed to normal porphyrin decay from residual $DTE_o\text{-P}$ dyad.

excitation 650 nm with constant irradiation at ~312 nm and probe at 700 nm

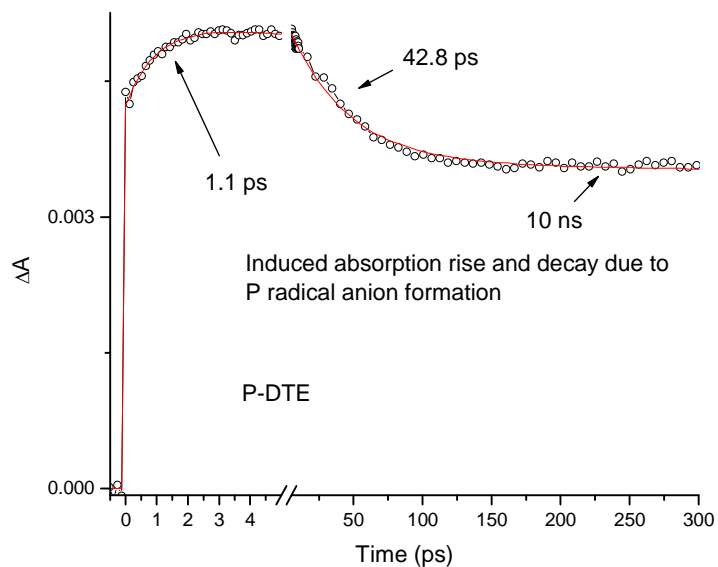


Figure 5. Transient absorption kinetic plot of dyad DTE_c-P

The absorption spectra for Triad 1 shows absorption maximas at 421 (Soret), 514, 549, 593, and 650 nm for triad DTE_o-P-C₆₀ and 423 (Soret), 515, 550, 651 nm for triad DTE_c-P-C₆₀ shown in Figure 6 .

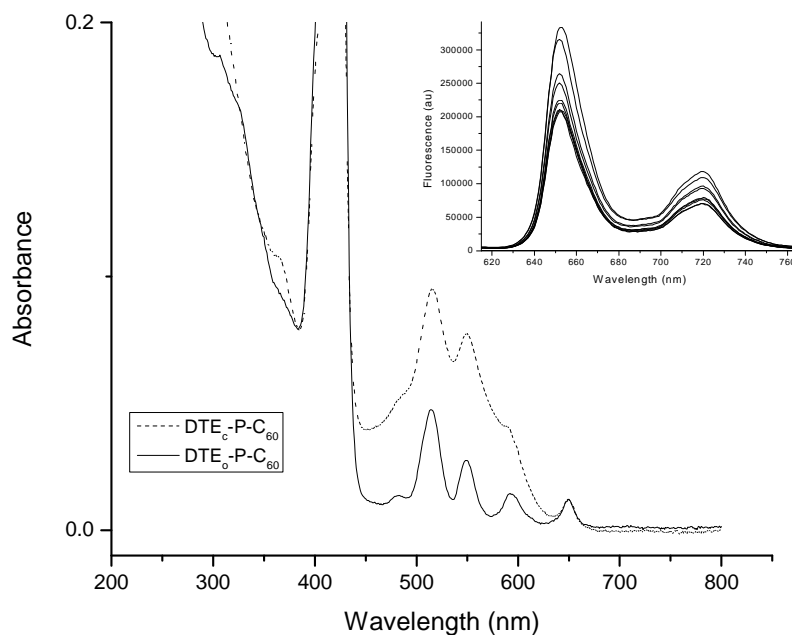


Figure 6. UV-vis Absorption and Emission Scans of Triad 1

Both isomers have absorption throughout the visible region due to the fullerene moiety with its long wavelength maximum at 710 nm. As seen in the absorption spectra, the visible region is not affected by the addition of DTE_o; however in triad DTE_c-P-C₆₀ an increase in absorbance is observed in the 550 nm region. The porphyrin absorbance is superimposed upon this band. This leads to the conclusion that DTE isomerization occurs in Triad 1. The emission scans from steady state fluorescence shown in Figure 6 inset, show a decrease in fluorescence as DTE_o is photoisomerized to DTE_c. These porphyrin fluorescence intensities are comparable to what was observed in dyad 2.

Time-resolved fluorescence measurements of triad DTE_c-P-C₆₀ required two exponentials, with time components of 43 ps, and 1.9ns, shown in Figure 7 inset.

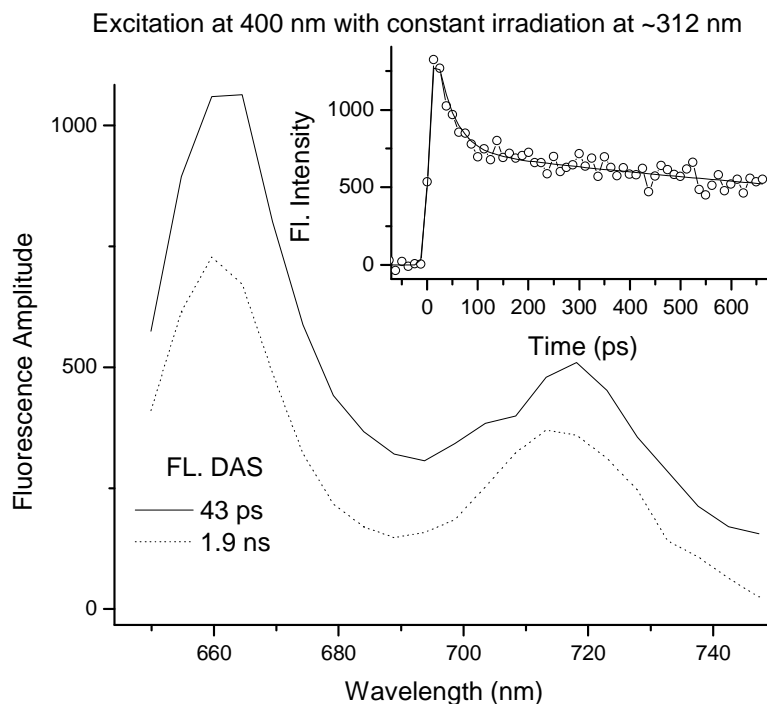


Figure 7. Time Resolved Fluorescence of Triad 2

The 43ps time component was ascribed to triad $\text{DTE}_c\text{-P-C}_{60}$, and the 1.9ns component was ascribed to triad $\text{DTE}_o\text{-P-C}_{60}$. Thus, the time resolved fluorescence indicates quenching of the porphyrin first excited state by DTE_c . Literature indicates that when DTE is in the open form, the 1.9ns²³ component is caused by photoinduced electron transfer between the porphyrin first excited state to the fullerene moiety to yield $\text{DTE-P}^+\text{-C}_{60}^-$.

The charge separation process was further studied using transient absorbance using 100fs laser pulses at 650nm under constant UV irradiation (~312 nm). Figure 8 shows the transient absorption spectrum at 1000nm showing four exponential components, with time constants of 1.1 ps, 42.8 ps, 1.9 ns, and 4.8 ns. As seen in dyad 2 the 1.1ps component was ascribed to the decay of $\text{DTE}_c^+\text{-P}^-\text{-C}_{60}$, while the 42.8 ps decay was attributed to the formation of $\text{DTE}_c^+\text{-P}^-\text{-C}_{60}$ charge separated states. The 1.9 ns time component was ascribed to formation of $\text{DTE-P}^+\text{-C}_{60}^-$

charge separated state, with the 4.8 ns component ascribed to the decay of that charge separated state.

excitation 650 nm with constant irradiation at ~312 nm and probe at 1000 nm

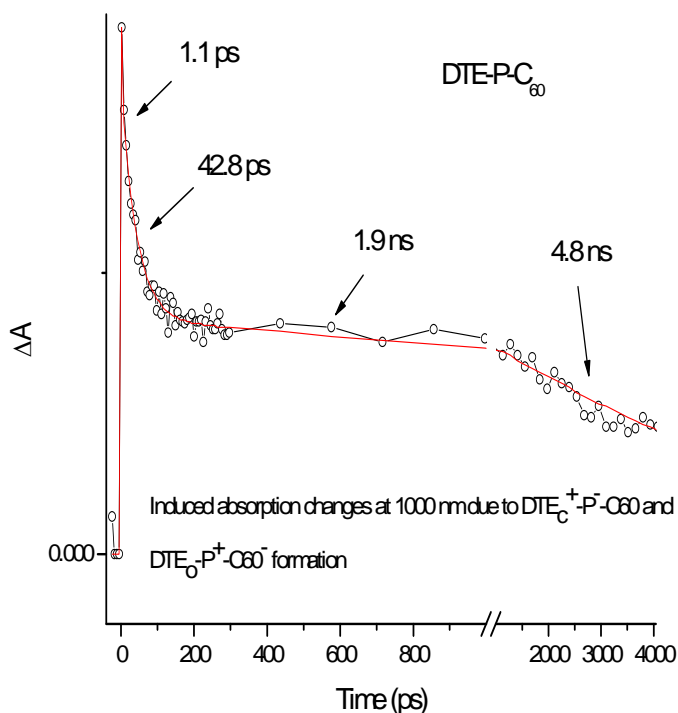


Figure 8. Transient Absorbance of Triad 2

Energetics. Estimated energies of various excited states and charge separated states are needed to interpret the results. The porphyrin and DTE_c first excited singlet state energies, estimated from the wavenumber average of the longest wavelength absorption maximum and the shortest wavelength emission band, were 1.92 and 2.13 eV above the ground state, respectively. Due to limited availability of triad 1 and dyad 2, redox potentials were taken from literature^{21,23} and used to estimate the charge separated state energies. The first oxidation potential of the model porphyrin in acetonitrile is 1.04 V versus SCE, while its first reduction potential is -0.99 V versus SCE. The first reduction potential of fullerene model is -0.99 V versus SCE. The first oxidation potential of DTE_c is 0.37 versus SCE, thus the of DTE_c⁺-P⁻-C₆₀ state is estimated at

1.36 eV above the ground state, and the $\text{DTE-P}^+-\text{C}_{60}^-$ state is estimated at 1.62 eV above the ground state. Using these data an energy diagram showing the energetics of various states of triad **1** and their inter-conversion pathways are shown in figure **9**.

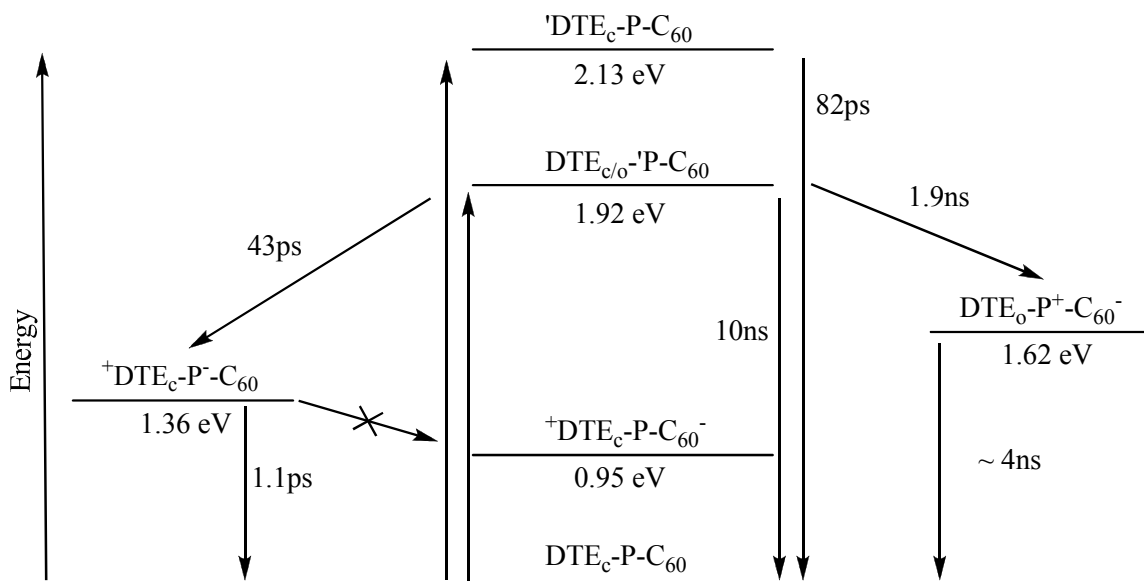


Figure 9. Energy Level Diagram of Triad **1**

Conclusions. In the open, dithienylethene form excitation of the porphyrin moiety of DTEH-P dyad **2** in 2-methyltetrahydrofuran is followed by deactivation of singlet excited state by usual photophysical processes of internal conversion, intersystem crossing and fluorescence ($\tau = 10$ ns). This implies that attachment of the DTEH_o moiety does not affect the porphyrin excited state. Irradiation of dyad **2** with UV light (~ 312 nm) photoisomerizes the dithienylethene moiety to its open form, which is much easier to oxidize. Excitation of the porphyrin moiety in $\text{DTE}_c\text{-P}$ dyad results in rapid photoinduced electron transfer from the DTE_c to the porphyrin leading to the formation ($\tau = 43$ ps) of $\text{DTE}_c^+-\text{P}^-$ charge separated state with a lifetime of 1.1 ps.

When the DTE moiety is in the open, colorless state (DTEH_o) excitation of the porphyrin chromophore leads to photoinduced electron transfer to the C_{60} moiety to yield the $\text{DTE}_o\text{-P}^+-\text{C}_{60}^-$ charge separated state with a lifetime of 4 ns. Irradiation of triad **1** with UV light (~ 312 nm)

isomerizes DTEHo to the closed, colored state (DTEHc). In this form, the porphyrin excited state, is quenched by electron transfer to yield $\text{DTE}_c^{\cdot+}\text{-P}^{\cdot-}\text{-C}_{60}$ charge separated state with a lifetime of 1.1 ps. The quantum yield of this process is approximately 40% due to an unfavorable photostationary state. Final charge separated state $\text{DTE}_c^{\cdot+}\text{-P-C}_{60}^{\cdot-}$ is energetically possible, but extremely short lifetime of $\text{DTE}^{\cdot+}\text{-P}^{\cdot-}$ hinders further electron transfer. Irradiation of DTEHc with visible light ($\lambda > 500\text{nm}$) returns the DTE moiety to its open form. Due to the high redox potential of the first reduction of DTE_c , it is energetically unfavorable to form the $\text{DTE}_o^{\cdot-}\text{-P}^{\cdot+}\text{-C}_{60}$ state. Inserting a larger insulator between DTE and porphyrin moieties, could result in a slower recombination $\text{DTE}_c^{\cdot+}\text{-P}^{\cdot-}\text{-C}_{60}$ state, thus allowing for final charge separated state $\text{DTE}_c^{\cdot+}\text{-P-C}_{60}^{\cdot-}$.

CHAPTER 3

PHOTOCHROMIC MODULATION OF FLUORESCENCE

Molecular Design. Light absorption by chromophores, yields an electronic excited state.

The chromophore usually returns to its electronic ground state, from its initial electronic excited state, a lower electronic excited state, or energy transfer to another chromophore, resulting in fluorescence. These competing processes and other chromophores present that absorb and emit in the same region can cause problems when fluorescence is used for imaging in biomedical or other applications.

Photochromic molecules are a special class of compounds that have two metastable isomeric forms, which can be reversibly converted between both states with light or sometimes heat. Due to these properties photochromes covalently attached to chromophores have been used as a switch to control energy transfer or photo-induced electron transfer in molecular systems.^{18,19, 24}

Keirstead et al. reported a system in which autofluorescence problems can be theoretically eliminated.²⁵ Fluorescence of a bis(phenylethynyl)anthracene (BPEA) chromophore was controlled by singlet-singlet energy transfer to a dithienylethene (DTE) photochromic switch, which photoisomerizes from its open colorless form to its colored closed form using UV light. Modulation of fluorescence was shown by sine and square wave modulation of red light, however there were some complications associated with this system. First, photoisomerization of DTE was slow resulting in modulation periods of several hundreds of seconds, making phase-sensitive detection difficult. Second, UV light was required in order to keep a sufficient population closed DTE isomer. The use of UV light rapidly decomposed the compound, especially in the presence of oxygen.

In order to eliminate these problems a spiro[azahomoadamantane-phenanthrolioxazine](SO)- BPEA dyad was synthesized. While most photochromes are colorless in their electronic ground state the spiro[azahomoadamantane-phenanthrolioxazine] photochrome used is colored in its electronic ground state and rapidly converts back to its colorless isomer thermally. In the closed form, fluorescence is strongly quenched by singlet-singlet energy

transfer, which isomerizes the photochrome to its closed colorless state. A population of closed photochromes allows for strong fluorescence of the BPEA moiety. Further modulation can be achieved by closing the photochrome using light, and exciting the BPEA moiety.

Synthesis. Dyad 18 was synthesized according to the route seen in Figure 21. **10** was afforded by alkylation of bromobenzene with commercially available 5-hydroxyadamantan-2-one and trifluoromethanesulfonic acid. **10** was then treated with methymagnesium iodine to obtain **11**. Treatment of **11** with sodium azide resulted in ring expansion and compound **12**. 9-bromoanthraldehyde was coupled to 4-*tert*-butylphenylacetylene via the Sonogoshira reaction to afford **14**. **14** was treated with dimethyl-(1-diazo-2-oxopropyl) phosphonate to yield **15**. **12** and **15** were then coupled using palladium coupling reagents. **16** was treated with methyl iodide yielding **17**, which was then coupled to 5-hydroxy-6-nitroso-1,10-phenanthroline to yield dyad **18** using previously described methods.²⁶

Photochemistry. Figure 10 shows that the absorption spectrum of **20** (SO) is highly dependent of solvent. In acetonitrile, solvent polarity stabilizes zwitterionic **21** (PMC) leading to a strong absorbance at 547 nm, with absorbance maxima at 334, 360 (sh), 465(sh), and 515(sh) nm. Absorbance maxima for model **19** are 312, 439, and 464 nm.

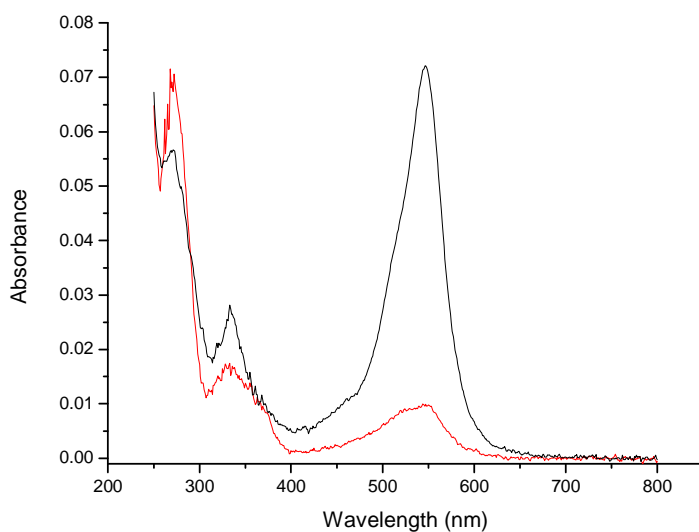


Figure 10. Absorption spectra of **20** in acetonitrile (red) and cyclohexane (black)

Absorbance maxima for dyad **18** are 313, 333, 441, and 515 (sh), and 549 nm, thus the spectrum for dyad **18** is essentially the sum of **20_o** and **19** absorption spectra, shown in Figure 11. In cyclohexane, the peak at 547 nm largely disappears in cyclohexane due to conversion of **20** to **21**, which has absorption at 255 and 350 nm. This same effect can be seen in **18**, thus dyad **18** exists in mostly its zwitterionic isomer in acetonitrile. Excitation of BPEA (mostly) at 400nm in **18** results in a fluorescence spectrum with maxima at 478, 508, and 545 (sh) nm, which arise from BPEA emission of BPEA-SO isomer also shown in figure 11.

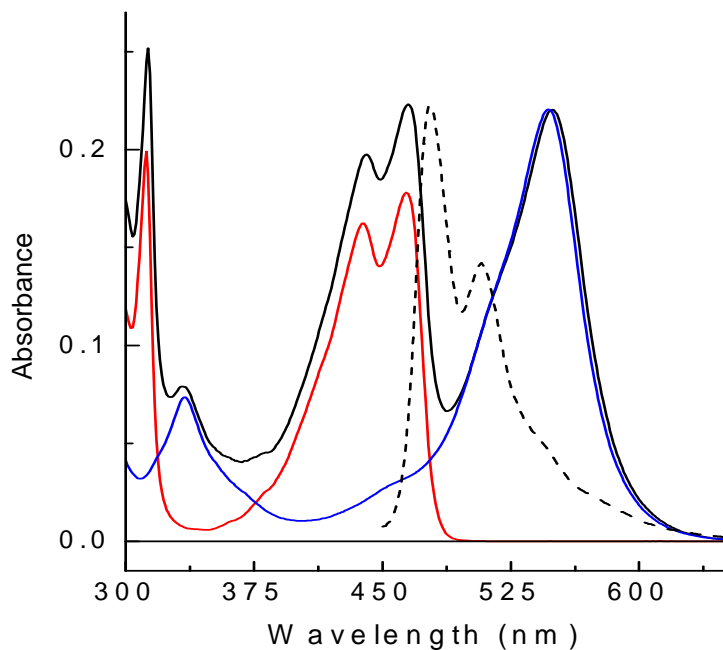


Figure 11. Absorbance spectra of model BPEA (red), **18** (black), and **20** (blue) in acetonitrile. Emission spectra of **18** in acetonitrile (dashed)

Fluorescence lifetimes were investigated and calculated by time-resolved methods by using single photon counting method. **19** in acetonitrile was excited at 475 nm, monitoring the emission at 560nm yielding a single exponential decay with a time constant of 3.68 ns ($\chi^2 = 1.10$).

Under the same conditions **18**, showed two time constants of 85 ps (11% of the decay) and 2.80 ns (89%, $\chi^2 = 1.16$). Since most of **18** is in the SO form, (~95%) in acetonitrile, these time constraints were attributed to the open form of dyad **18**. Due to these time constants being smaller than that of **19**, quenching of the singlet excited state of BPEA from SO is confirmed. An amplitude-weighted singlet state lifetime of 2.5 ns for BPEA in **18** was calculated. From this and the fluorescence lifetime of model BPEA, the average rate constant of quenching of BPEA excited singlet state (k_q) can be calculated using equation 3, where τ_{obs} is the lifetime of the BPEA excited state in dyad **18** and τ_m is the fluorescence lifetime of the BPEA model **19**.

$$k_q = \frac{1}{\tau_{obs}} - \frac{1}{\tau_m} \quad (3)$$

The quantum yield of quenching (0.32) can be calculated using equation 4,

$$\Phi_q = k_q \tau_{obs} \quad (4)$$

where $k_q = 1.28 \times 10^8 \text{ s}^{-1}$ calculated from above.

Modulation of Fluorescence. The above experiments show that fluorescence quenching of BPEA moiety occurs in **18** when the photochromic moiety is in the open form and that the quantum yield of fluorescence was reduced by 32%. Fluorescence quantum yield should be able to be increased by irradiation of the SO moiety in **18**. In order to test this, **18** was irradiated with low-intensity blue light 440 nm at 300 K, to promote BPEA fluorescence, which was monitored at 480 nm. The sample was also irradiated from 550 nm to 610 nm by passing a white laser through a prism monochromoter, and a 570 nm long pass filter. Two different experiments were done to achieve modulation. The first experiment involved generation of a square wave using a mechanical chopper giving light at 0 or 10 mW/cm². The results for modulation using square wave can be seen in figure 12.

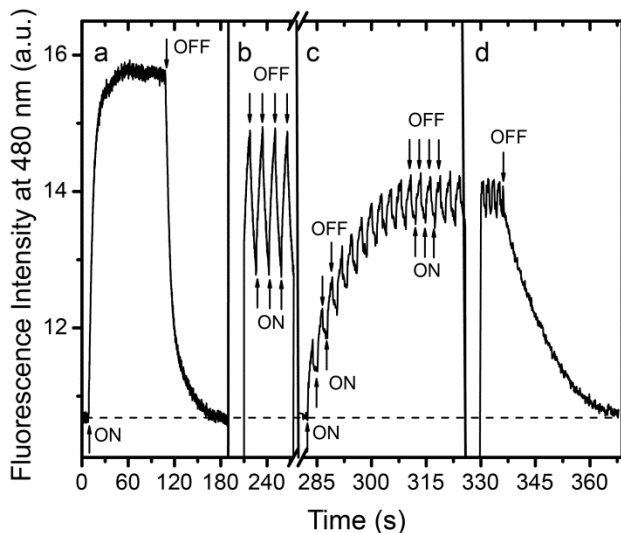


Figure 12. Square wave modulation of Fluorescence of **18**

Part A of the experiment shows one cycle of modulation, with a period of 200s. BPEA fluorescence is achieved by constant irradiation with 440 nm light. When the yellow light is turned on, fluorescence intensity increases due to photoisomerization of SO to PMC forms. Due to fast thermal relaxation fluorescence activity returns to zero relatively quickly. In part B, square wave function is reduced to 16 s. Square wave form is no longer observed, but a saw tooth wave form is observed. Modulation intensity is lower since the sample does not have time to reach a steady state distribution. In part C, the square wave period is reduced to 9.4 s. The same saw tooth wave form is observed however average amplitude of fluorescence increase until a photostationary state distribution of SO and PMC is reached. In part D, fluorescence is returned to its initial value as the yellow light is switched off. This is due to thermal equilibrium being reached between open and closed forms.

The results of sine wave modulation using yellow light, with a period of 50 s, on BPEA fluorescence in **18** can be seen in figure **13**.

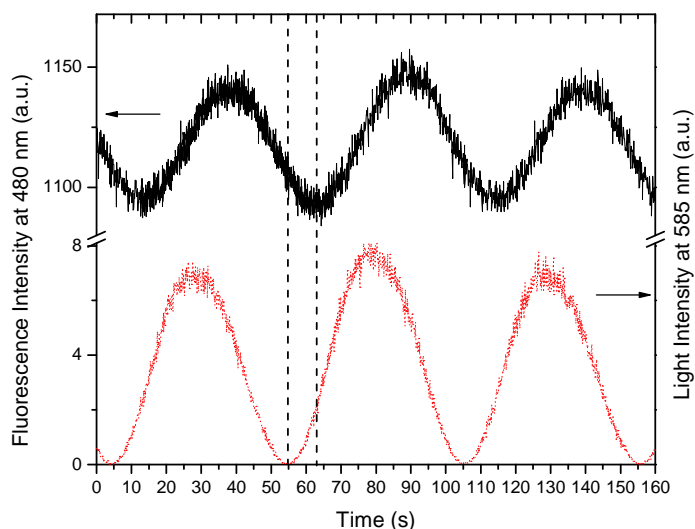


Figure 13. Sine wave modulation of BPEA fluorescence in **18** (black). Sine wave modulated light used (red).

A small phase shift occurs, shown by two vertical black lines, due to photoisomerization of the photochrome not keeping up with modulation.

Energetics. Estimated energies of various excited states and charge separated states are needed to interpret the results. The BPEA first excited singlet state energies, estimated from the wavenumber average of the longest wavelength absorption (465 nm) maximum and the shortest wavelength emission band (478 nm), is 2.63 eV. Redox potentials were investigated from cyclic voltammetric measurements. Studies were carried out using 0.1M tetra-*n*-butylammonium hexafluorophosphate, in acetonitrile using a glassy carbon working electrode. The first reduction and oxidation potentials of model BPEA are -1.33 and 1.17 respectively. From this we can determine the first oxidation and first reduction potentials of BPEA and SO in **18**. The first oxidation and reduction potential for SO in **18** are 0.69 and -0.97 V versus SCE respectively, while the first oxidation and reduction potentials for BPEA in **18** are 1.20 and -1.36 V versus SCE. Calculated from the redox potentials mentioned above a BPEA^{•+}-SO^{•-} state is 2.17 eV above the neutral state. A BPEA⁻-SO^{•+} state would lie at 2.05 eV above the neutral state, thus

photoinduced electron transfer is thermodynamically possible but due to significant overlap of absorption and emission spectra singlet-singlet energy transfer from BPEA to SO is likely.

Conclusion. Dyad **18** exhibits the properties it was designed for. In its electronic ground state, SO in **18** remains in its colored zwitterionic open isomer, and can be photoisomerized to the closed form using yellow/red light, which thermally isomerizes back to its colored form rapidly. BPEA fluorescence is strongly quenched when SO is in the colored form, and exhibits strong fluorescence in the open form. Blue fluorescence can be modulated by photoisomerizing SO to the closed form. This ability to modulate fluorescence can be used in fluorescence imaging detection experiments without interference from “autofluorescence” or other adventitious light.

CHAPTER 4

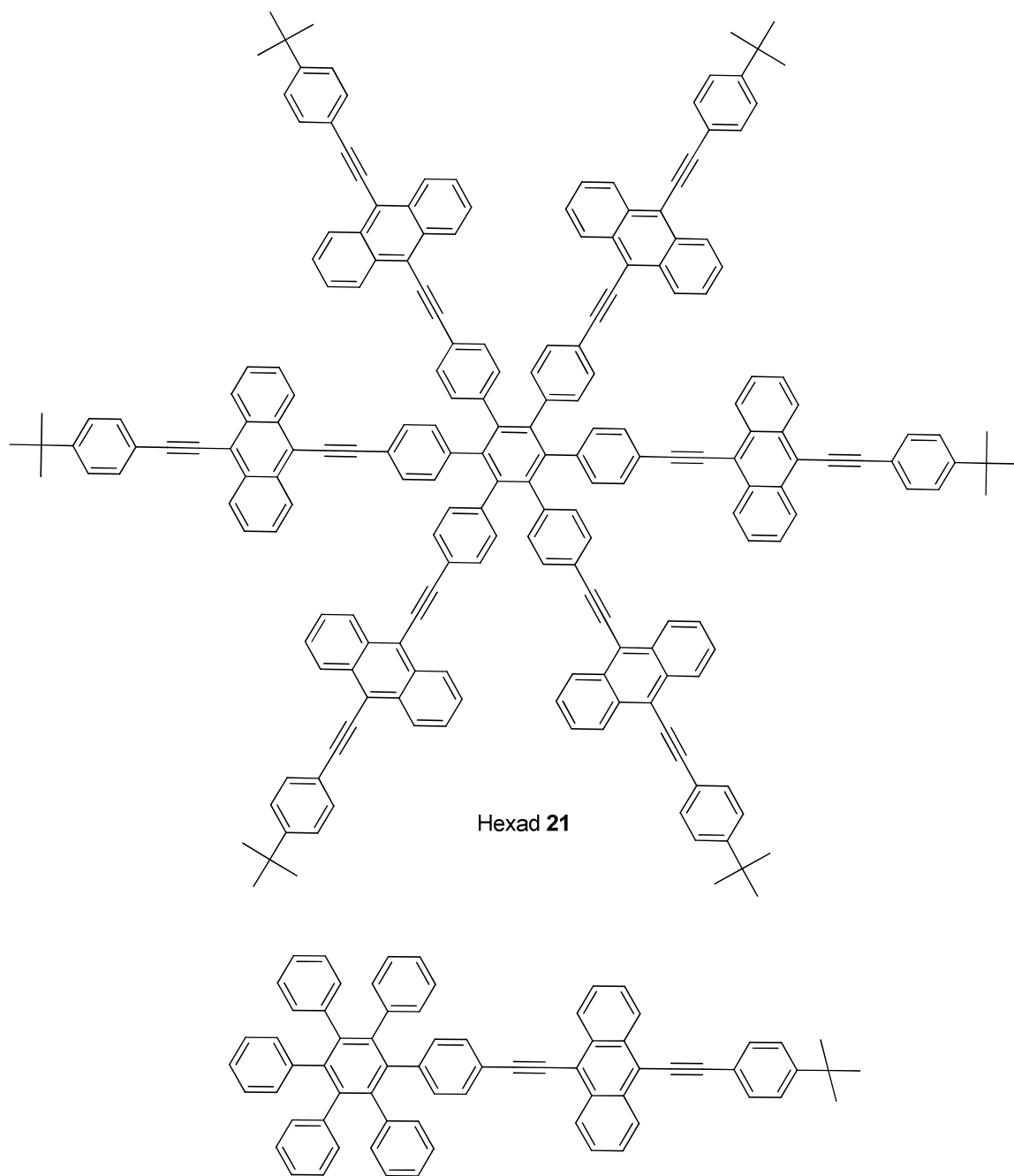
COVALENTLY ATTACHED FLUOROPHORES IN A TRIPLET-TRIPLET ANNIHILATION UPCONVERSION SYSTEM

Introduction. Arguably, one of the greatest challenges facing mankind today is the implementation of a carbon neutral energy source. Since the industrial age began, the combustion of fossil fuels has improved the standard of living for a significant portion of the global population. However, fossil fuel supplies are limited, and their combustion is clearly linked with ongoing changes to our planet's climate system. Energy demand will be increased due to simple economics, along with humans needs and desires.²⁷ Recent estimations have shown that by the year 2030 the world's energy demand will have increased by 57% from 14.9 terawatt (TW) to 23.4 TW.²⁸ Achieving this will require research into all types of energy, but very likely coal will be used as the primary source for this energy, causing global consequences. The innovation and implementation of renewable energy is inevitable in order to reduce the amount of anthropogenic carbon dioxide emissions. Solar energy hits the surface of the earth at a rate of 120,000 TW,² far above the demand of 14.9 TW of global human energy demands.³ Clearly solar energy can provide enough energy for human demands making solar energy a favorite future energy source .²⁹

Solar energy utilization can be accomplished by many ways, however photovoltaic cells are the most commonly used solar energy. Photon absorption by the silicon semiconductor leads to excitation migration to the p-n junction where charge separation occurs. Charge separation generates electromotive forces, forcing current flow through a wire, where decay to the ground state is prevented by the intrinsic electric field.³⁰ However, due to high cost of photovoltaic solar cells their use is limited.

Attempts by human efforts to capture the suns energy into a more useable form is loosely known as artificial photosynthesis. Artificial photosynthesis can provide a cheaper alternative to silicon based photovoltaics, but the efficiency is greatly reduced. One way to overcome this obstacle is to use the entire solar spectrum, most notably the red portion. One way this goal can

be achieved is by synthesizing red absorbing dyes covalently attached to an electron acceptor to achieve charge separation. This approach has proved to be synthetically problematic. In order to use the red portion of the solar spectrum, this work used triplet-triplet annihilation upconversion (TTA-UC) to absorb red photons, and emit green photons. TTA-UC is a three step process. The first step requires a dye to absorb light and initiate a triplet excited state, followed by energy donation to an emitter. The final step requires one triplet emitter to donate its energy to another triplet emitter, resulting in a single singlet excited state, which then emits by normal fluorescence pathways. Triplet-triplet annihilation upconversion itself is plagued by low quantum yield. To improve TTA-UC one of the diffusion steps was eliminated by covalently attaching 6 bisphenylethynylantracene fluorophores to a hexaphenyl benzene core to create hexad **21**. Hexad **22** was then compared to monomer **21**.



Monomer **22**
Figure 14. Structure of Hexad **21** and Monomer **22**

Synthesis. Synthesis of hexad **21**, shown in figure **22**, began by iodinating the para positions of hexaphenylbenzene with [bis(trifluoroacetoxy)iodo]benzene and iodine in dichloromethane followed a Sonogoshira coupling with the alkyne **15**. Synthesis of monomer **22**

was accomplished by Sonogoshira coupling (4-bromophenyl)pentaphenylbenzene with the alkyne **15**. The palladium porphyrin used was synthesized using known procedures.³¹

Photochemistry. The absorption spectra for hexad **21** and monomer **22** mixed with Porphyrin **23** are shown in figure **15**.

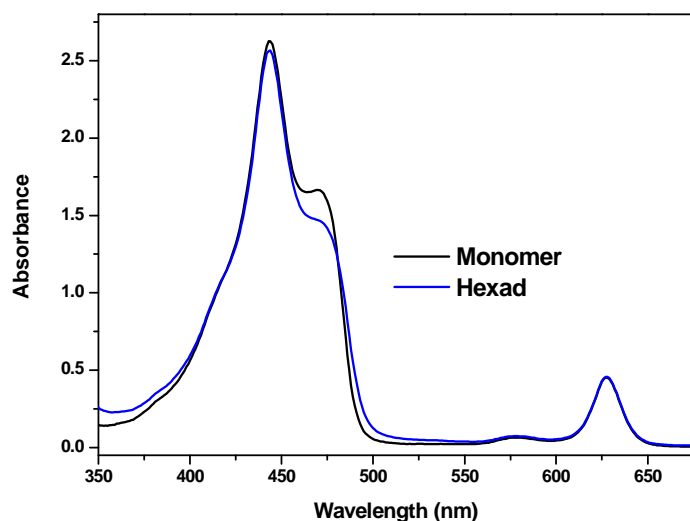


Figure 15. Absorbance Spectra of Monomer, Hexad, and Porphyrin mixed

The absorbance between 400 and 500 nm is due to hexad **21** and monomer **22** as well as the Soret of porphyrin **23**, while the absorbance at 628 nm is due to porphyrin **23**. Excitation of porphyrin **23** at 650 nm initiates TTA_UC. The emission spectra for hexad **21** and monomer **22** both at optical density of 0.1 and an optical density of 0.5 for porphyrin **23** can be seen in figure **16**.

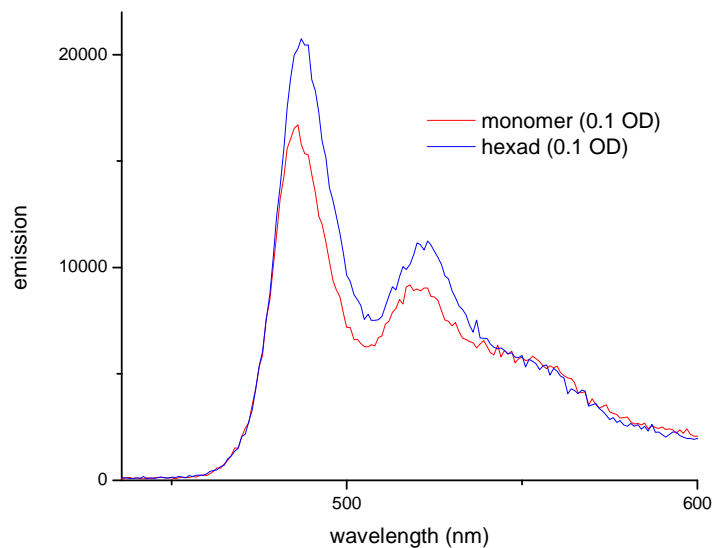


Figure 16. Emission spectra of TTA-UC

At equal optical density an increase in TTA-UC is observed. While the increase does not seem significant, the monomer is 6 times more concentrated. Thus, covalently attached fluorophores increase TTA-UC. While these results are interesting, under slightly aerobic conditions hexad **21** has a significant increase in TTA-UC over monomer **22**. This is due to the increased concentration of monomer **22** increases the likelihood of its ability to react with singlet oxygen.

Conclusion. Fluorescence intensity in a TTA-UC system was increased by covalently attaching fluorophores. This is caused by the reduction in one diffusion step. Although the quantum yield for this process is low, being able to utilize more of the solar spectrum with this system may improve the efficiencies of organic based solar conversion techniques.

CHAPTER 5

EXPERIMENTAL PROCEDURES

Experimental Procedures. In this final chapter, synthetic and characterization procedures for all novel compounds in previous chapters is described. Initial description of synthetic and characterization procedures and instrumentation will be given, divided by chapters. Additional characterization using unique spectroscopy will be described in that chapter. All reagents used were purchased from common commercial sources (Aldrich, TCI, etc.) and used without further purification unless otherwise noted. Solvents were used without further purification unless otherwise noted with the exception of THF and methyl THF which were distilled over sodium benzophenone and LAH, respectively.

General Instrumentation Techniques. ^1H NMR spectra were obtained using Varian Unity spectrometers at 300, 400, or 500 MHz. Samples were dissolved in deuterated chloroform using the residual solvent peak as an internal reference unless otherwise noted. Mass spectra were obtained on a matrix-assisted laser desorption/ionization time-of-flight spectrometer (MALDI-TOF). The solvent for all spectroscopy was freshly distilled methyl THF unless otherwise noted. All samples for spectroscopy were degassed by bubbling with argon for 20 minutes on ice, or freeze pump thaw techniques, then subsequently sealed in glass cuvettes described in the text. Ground state absorption spectra were obtained using Shimadzu UV-3101PC UV-vis-NIR spectrometer or a Shimadzu 2550 UV-visible spectrometer. Steady state fluorescence spectra were obtained using a Photon Technology International MP-1 fluorimeter and corrected. Excitation was produced by a 75 W xenon lamp and single grating monochromator. Fluorescence was detected at 90° to the excitation beam via a single grating monochromator and an R928 photomultiplier tube having S-20 spectral response operating in the single-photon-counting mode. Fluorescence decay measurements were performed on optically dilute (ca. 1×10^{-5} M) samples by the time-correlated single-photon-counting method. Two different systems were employed. Excitation source for the first system was a mode-locked Ti:Sapphire laser (Spectra Physics, Millennia-pumped Tsunami) with a 130-fs pulse duration operating at 80 MHz. The laser output

was sent through a frequency doubler and pulse selector (Spectra Physics Model 3980) to obtain 370-450 nm pulses at 4 MHz. Fluorescence emission was detected at the magic angle using a double grating monochromator (Jobin Yvon Gemini-180) and a microchannel plate photomultiplier tube (Hamamatsu R3809U-50). The instrument response function was 35-55 ps. The spectrometer was controlled by software based on the LabView programming language and data acquisition was done using a single photon counting card (Becker-Hickl, SPC-830). Fluorescence decay measurements were performed by the time-correlated single-photon-counting method (TC-SPC). The excitation source was a fiber supercontinuum laser based on a passive modelocked fiber laser and a high-nonlinearity photonic crystal fiber supercontinuum generator (Fianium SC450). The laser provides 6-ps pulses at a repetition rate variable between 0.1 – 40 MHz. The laser output was sent through an Acousto-Optical Tunable Filter (Fianium AOTF) to obtain excitation pulses at desired wavelength. Fluorescence emission was detected at the magic angle using a double grating monochromator (Jobin Yvon Gemini-180) and a microchannel plate photomultiplier tube (Hamamatsu R3809U-50). The instrument response function was 35-55 ps. The spectrometer was controlled by software based on the LabView programming language and data acquisition was done using a single photon counting card (Becker-Hickl, SPC-830). Transient absorbance measurements were performed on a femtosecond transient absorption apparatus consisting of a kilohertz pulsed laser source and a pump-probe optical setup. Laser pulses of 100 fs at 800 nm were generated from an amplified, mode-locked Titanium Sapphire kilohertz laser system (Millennia/Tsunami/Spitfire, Spectra Physics). Part of the laser pulse energy was sent through an optical delay line and focused on to a 3 mm sapphire plate to generate a white light continuum for the probe beam. The remainder of the pulse energy was used to pump an optical parametric amplifier (Spectra Physics) to generate excitation pulses, which were selected using a mechanical chopper. The white light generated was then compressed by prism pairs (CVI) before passing through the sample. The polarization of pump beam was set to the magic angle (54.7°) relative to the probe beam and its intensity adjusted using a continuously variable neutral density filter. The white light probe is dispersed by a spectrograph (300 line grating) onto a charge-coupled device (CCD) camera (DU420, Andor

Tech.). The final spectral resolution was about 2.3 nm for over a nearly 300 nm spectral region. The instrument response function was ca. 150 fs. The nanosecond-millisecond transient absorption measurements were made with excitation from an optical parametric oscillator driven by the third harmonic of a Nd:YAG laser (Ekspla NT342B). The pulse width was ~4-5 ns, and the repetition rate was 10 Hz. The detection portion of the spectrometer (Proteus) was manufactured by Ultrafast Systems. The instrument response function was ca. 4.8 ns.

Experimental for Chapter 2. Closing and opening of the DTE moiety in triad 1, dyad 2, and model photochrome 3 were accomplished by using, a UVP UV lamp Model UVGL-25 and white light from a tungsten 160 W light, using a long pass filter to eliminate shorter wavelengths shorter than 500 nm

Using previously described methods 1,2-bis(5-chloro-2-methylthiophen-3-yl)cyclopent-1-ene **5** was prepared and converted to 5-chloro-3-(2-(5-(4-methoxyphenyl)-2-methylthiophen-3-yl)cyclopent-1-en-1-yl)-2-methylthiophene **6**.²¹

Porphyrin 7. A flask containing 4'-bromobiphenyl-4-carbaldehyde (210 mg, 0.80 mmol), methyl 4-formylbenzoate (.132 g, 0.80mmol), *Meso*-(mesityl)dipyrromethane (0.4246 g, 1.6 mmol), and chloroform (160 mL) was flushed with argon for 20 min. $\text{BF}_3 \cdot \text{OEt}_2$ (70.6 μl , 0.56 mmol) was added dropwise, and the solution was allowed to stir for 6 hours. 2,3-Dichloro-5,6-dicyanoquinone (0.45 g, 1.98 mmol) was added, and stirring was continued overnight. The solution was filtered through silica (dichloromethane), and the solvent was removed under reduced pressure. The residue was purified by column chromatography on silica (dichloromethane/hexanes: 8/2), and crystallized (dichloromethane/methanol) to yield small purple crystals (200 mg, 27%). ^1H NMR (400MHz, CDCl_3) δ = -2.61 (s, 2H), 1.84 (s, 12H), 2.63 (s, 6H), 4.11 (s, 3H), 7.285 (s, 4H), 7.71 (d, 2H, J = 8.5 Hz), 7.78 (d, 2H, J = 8.5 Hz), 7.93 (d, 2H, J = 8.1 Hz), 8.29-8.32 (t, 4H), 8.42 (d, 2H, J = 8.1 Hz), 8.71-8.74 (m, 6H), 8.86 (d, 2H, J = 4.8 Hz) ppm.

Dyad 2. A solution of *n*-BuLi (93 μ L of 2.5 M solution in hexanes, 0.233 mmol) was added dropwise at room temperature to a flask containing **6** (0.0593 g, 0.148 mmol) dissolved in anhydrous THF (10 ml). After 1 hour of stirring B(OBu)₃ (0.087 ml, 0.0321 mmol) was added, and the mixture was stirred for an additional 2 hours. In a separate flask, **7** (125 mg, 0.14 mmol) dissolved in THF (10 mL), Pd(PPh₃)₄ (8 mg, 5 mol%), aqueous Na₂CO₃ (1 ml, 2 M), and ethylene glycol (3 drops), were heated to reflux, and the solution from above was added drop wise using a syringe, and refluxed for 48 h. Acetic acid (2 mL) and water (25 mL) were added to the cooled solution, and the aqueous phase was extracted with diethyl ether (3 x 50 ml). The combined organic phases were washed with water (1 x 50 mL), dried (MgSO₄), filtered, and the solvent was removed under reduced pressure. The residue was purified by column chromatography on silica (freshly distilled hexanes/ethyl acetate: 95/5) to yield a purple powder (16 mg, 9.5%). ¹H NMR (400MHz, CDCl₃) δ = -2.60 (s, 2H), 1.85 (s, 12H), 2.05 (d, 6H, *J* = 7.7 Hz), 2.12 (t, 2H), 2.63 (s, 6H), 2.88-2.90 (m, 4H), 3.83 (s, 3H), 4.11 (s, 3H), 6.89 (d, 2H, *J* = 8.6 Hz), 6.96 (s, 1H), 7.18 (s, 1H), 7.28 (s, 4H), 7.45 (d, 2H, *J* = 8.6 Hz), 7.71 (d, 2H, *J* = 8.4 Hz), 7.88, (d, 2H, *J* = 8.2 Hz), 7.98 (d, 2H, *J* = 8.2 Hz), 8.28-8.32 (m, 4H), 8.42 (d, 2H, *J* = 8.2 Hz) 8.70-8.74 (m, 6H), 8.88 (d, 2H, *J* = 4.6 Hz) ppm. MALDI-TOF-MS *m/z* = calculated for C₈₀H₆₈N₄O₃S₂ 1196.47, observed 1196.52. UV/Vis (dichloromethane) λ_{\max} = 420, 515, 551, 590, 648 nm.

Dyad 3. A flask containing dyad **2** (10.9 mg, 0.0091 mmol) dissolved in THF (20 mL), methanol (10 ml), and 10% aqueous KOH (5 mL) were refluxed for 48 hours. The cooled solution was extracted with dichloromethane (2 x 25 mL), and the combined organic phases were dried (MgSO₄), filtered, and the solvent was removed under reduced pressure. The residue was purified by column chromatography on silica (freshly distilled dichloromethane/methanol: 97/3) to yield a purple powder in essentially quantitative yields. ¹H NMR (500 MHz, CDCl₃) δ = -2.62 (s, 2H), 1.83 (s, 12H), 2.03 (d, 2H, *J* = 9.5 Hz), 2.08-2.12 (m, 2H), 2.61 (s, 6H), 2.87 (m, 4H), 3.81 (s, 3H), 6.88 (d, 2H, *J* = 8.7 Hz), 6.94 (s, 1H), 7.16 (s, 1H), 7.27 (s, 4H), 7.44 (d, 2H, *J* = 8.6 Hz), 7.70 (d, 2H, *J* = 8.2 Hz), 7.88 (d, 2H, *J* = 8.3 Hz) 7.97 (d, 2H, *J* = 8.3 Hz), 8.27 (d, 2H, *J* = 8.0 Hz), 8.33 (d, 2H, *J* = 8.0 Hz), 8.47 (d, 2H, *J* = 8.0 Hz), 8.69-8.74 (m, 6H), 8.87 (d, 2H, *J* = 4.7 Hz) ppm.

Triad **1**. A flask containing dyad **3** (9 mg, 0.0076 mmol) dissolved in dichloromethane (5 ml), EDCI (3 mg, 0.015 mmol), 4-dimethylaminopyridine (2 mg, 0.02 mmol), and **8** (8 mg, 0.0092 mmol) were stirred overnight under an argon atmosphere. The solution was extracted with dichloromethane (3 x 25 mL), and the combined organic phases were dried (MgSO₄), filtered, and the solvent was removed under reduced pressure. The residue was purified by column chromatography on silica (freshly distilled toluene/dichloromethane: 6/4) to yield a purple powder (3.6 mg, 23%). ¹H NMR (400 MHz, CDCl₃), δ = -2.67 (s, 2H), 1.78 (s, 12H), 1.98 (d, 6H, *J* = 7.9 Hz), 2.03-2.07 (m, 7H), 2.55 (s, 6H), 2.80-2.83 (m, 7H), 3.76 (s, 3H), 4.21 (d, 1H, *J* = 9.5 Hz), 4.92 (s, 1H), 4.94 (d, 2H, *J* = 9.5 Hz), 6.82 (d, 2H, *J* = 8.6 Hz), 6.89 (s, 1H), 7.11 (s, 1H), 7.21 (s, 4H), 7.38 (d, 2H, *J* = 8.6 Hz), 7.64 (d, 2H, *J* = 8.4 Hz), 7.81-7.83 (m, 6H), 7.91, (d, 2H, *J* = 8.2 Hz), 8.12 (s, 1H), 8.15 (d, 2H, *J* = 8.2 Hz), 8.21 (d, 2H, *J* = 8.2 Hz), 8.26 (d, 2H, *J* = 8.2 Hz), 8.64-8.67 (m, 6H), 8.82 (d, 2H, *J* = 4.6 Hz) ppm. MALDI-TOF-MS *m/z* = calculated for C₁₄₈H₇₆N₆O₂S₂ = 2033.55, observed = 2033.69 UV/Vis (dichloromethane) λ_{max} = 420, 484, 516, 551, 599, 647, 705 nm.

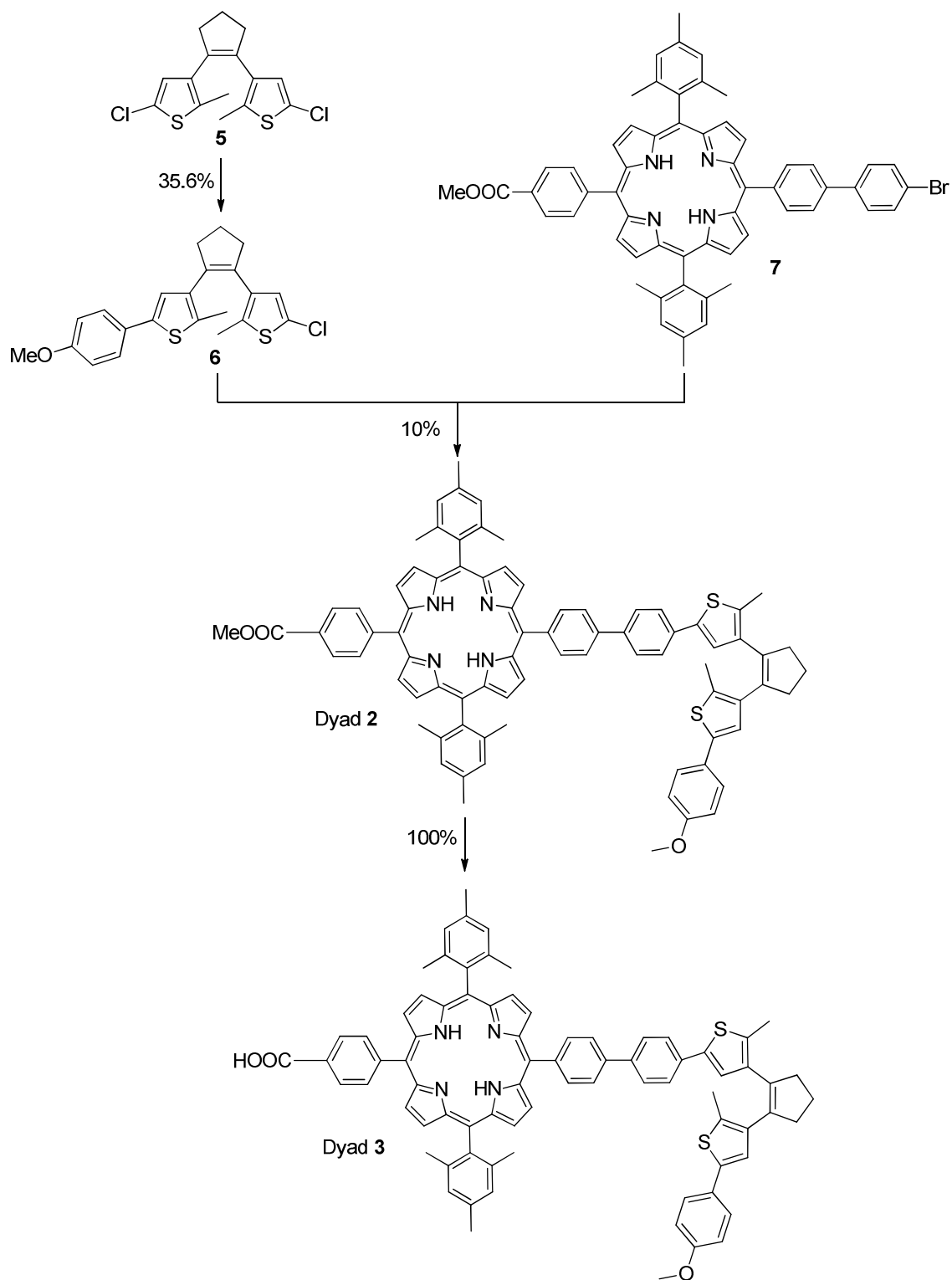


Figure 17. Synthetic scheme to obtain **Dyad 3**

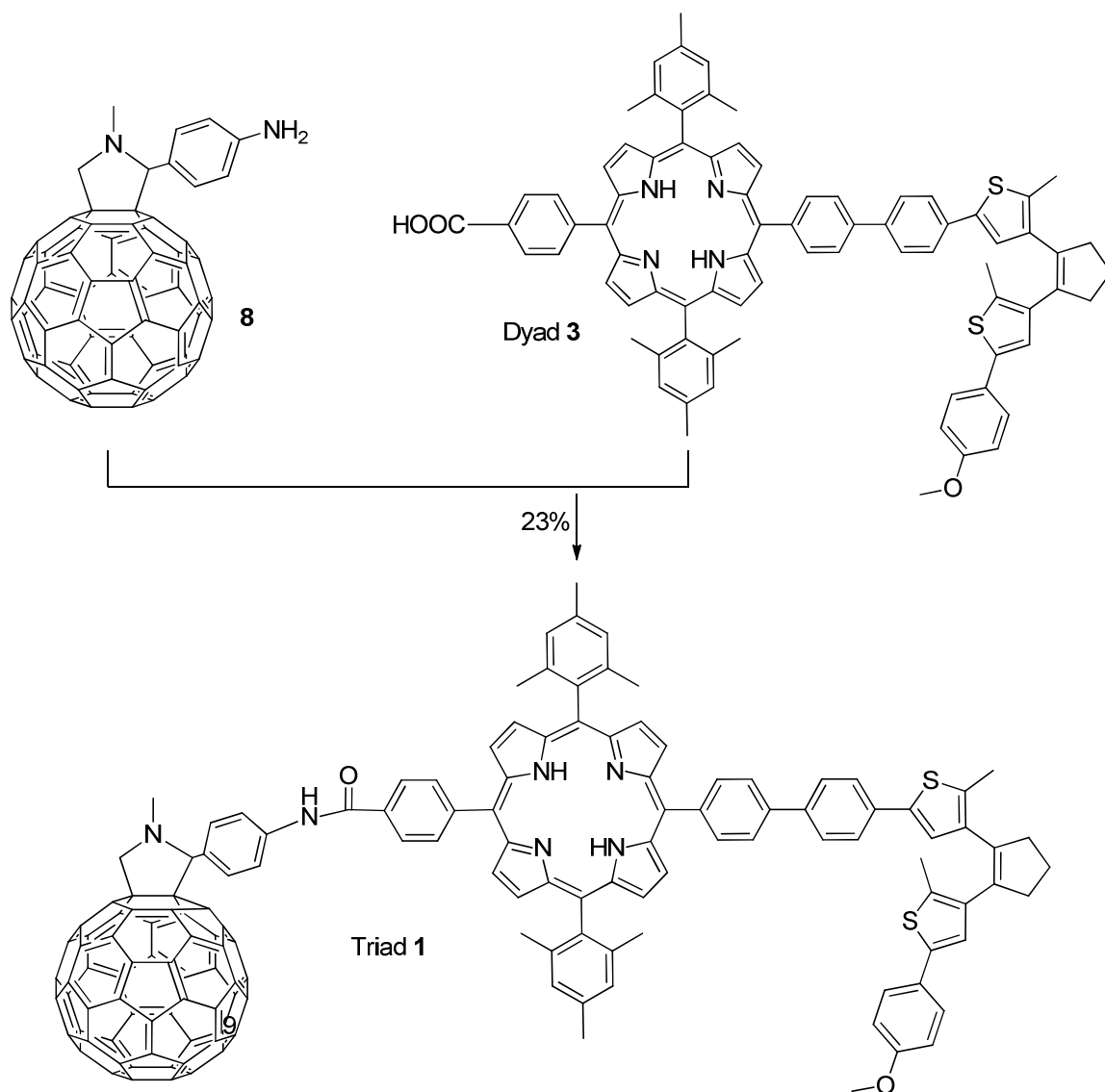


Figure 18. Synthetic scheme to obtain triad 1

Experimental for chapter 3. Photochromic switching between SO_c and SO_o isomers was achieved by excitation of BPEA at 440 nm as well as using a white laser passed through a monochromator prism and a 570 nm long pass filter. Reverse isomerization was achieved by thermal relaxation from the SO_c to SO_o isomers.

(1R, 3S, 5S, 7S)-5-(4-Bromophenyl)adamantan-2-one (**10**). 5-Hydroxyadamantan-2-one (**9**) (3.22 g, 19.36 mmol), bromobenzene (65 mL, 616.8 mmol) were added to a vigorously stirred 100 mL round bottom flask under an argon atmosphere at 0°C for 15 minutes. Triflic acid (1.1 mL, 12.4 mmol) was added via syringe without a needle in one portion, and stirred at 0°C for 30 minutes. The ice bath was removed and stirred at room temperature for 10 minutes, then heated to 95°C for 73 hours. The reaction was cooled to 0°C and NaHCO₃ (25 mL) was added, and the mixture was washed with additional NaHCO₃ (15 mL). The aqueous layer was extracted with ether (3 x 50mL), and the organic layers were combined and washed with water (1 x 100 mL), brine (2 x 75mL), dried (Na₂SO₄), and the solvent was removed under reduced pressure to yield a brown oily semi solid. The crude product was then stirred with 20 mL EtOAc/hexanes (18/82) over 3 days. The product was filtered and washed with an addition 5 mL EtOAc/hexanes (18/82) to yield 2.54 g (43%) of a white solid. ¹H NMR (400MHz CDCl₃) δ 2.15 (12H, m), 2.66 (2H, s), 7.22 (2H, d, *J* = 9 Hz), 7.45 (2H, d, *J* = 8.6 Hz) EI MS (M+) *m/z*: calcd for C₁₆H₁₇BrO 304, obsd 304.

(1R, 3S, 5S, 7S)-5-(4-bromophenyl)adamantan-2-one (**11**). 5-(4-Bromophenyl)adamantan-2-one (**10**) (3.06 g, 10.03 mmol) and THF (25 mL) were placed into a 3 neck round bottom flask under argon at 0°C. MeMgI (30 mL of a 1M solution) was added dropwise for 4 minutes, and stirred at 0°C for 2.5 hours. Saturated NH₄Cl (100 mL) was added and the mixture stirred for 5 minutes. Ether (100 mL), THF (50 mL), and water (150 mL) were added, and the aqueous layer was extracted with THF/ether (20/80, 2 x 100 mL) and ether (1 x 100 mL). The combined organic layers were combined, washed with water (2 x 150 mL), brine (1 x 150 mL), dried over anhydrous Na₂SO₄, and the solvent was removed under reduced pressure. The product was purified by recrystallization (hexanes) to yield 2.40 g (74.5%) of white opalescent plates. ¹H NMR (400MHz CDCl₃) δ 1.4 (3H, m), 1.43 (1H, br. s), 1.55 (1H, d, *J* = 12.9 Hz), 1.64 (1H, d, *J* = 12.5 Hz), 1.73 (1H, d, *J* = 12.1Hz), 1.84 (5H, m), 1.9 (2H, m), 2.04 (2H, m), 2.26 (1H, d, *J* = 12.5 Hz) 2.4 (1H, d, *J* = 12.1Hz), 7.23 (2H, m), 7.42 (2H, m) EI MS (M+) *m/z*: calcd for C₁₇H₂₁BrO 320, obsd 320.

(1S,3R,8R)-1-(4-Bromophenyl)-5-methyl-4-azatricyclo[4.3.1.1^{3,8}]undec-4-ene (**12**).

Dichloromethane (12mL) and methanesulfonic acid (18 mL) were added to a stirred round bottom flask at 0°C and cooled for 5 minutes. Sodium azide (0.6g, 9.22 mmol) was added and after 5 minutes 5-(4-bromophenyl)-2-methyladamantan-2-ol (**11**) (2.30 g, 7.16 mmol) was added. After 5 minutes of stirring additional sodium azide (1.19 g, 18.28 mmol) was added in portions over 25 minutes, then the reaction was stirred at room temperature overnight. Ice (15 g) was added, then KOH (30-35 mL 50% by weight/volume) was added to basify the solution to a pH \approx 10 when additional ice (20 g) was added. Water (100 mL) and dichloromethane (100 mL) were added and the aqueous layer was extracted with dichloromethane (4 x 100 mL). The combined organic layers were washed with water (1 x 200 mL), dried over Na₂SO₄, and the solvent was removed under reduced pressure to yield 2.25 g (97%) of an off- white solid. ¹H NMR (400MHz CDCl₃) δ 1.65 (5H, m), 1.78 (2H, m), 1.89 (1H, m), 1.98 (3H, m), 2.07 (3H, s), 2.38 (1H, quin, *J* = 7.1 Hz), 2.73 (1H, t, *J*=5.5 Hz), 4.16 (1H, spt, *J* = 4.9 Hz), 7.21 (2H, d, *J* = 8.6 Hz), 7.44 (2H, d, *J* = 8.6 Hz).

10-((4-(*tert*-Butyl)phenyl)ethynyl)anthracene-9-carbaldehyde (**14**) . 9-Bromoanthraldehyde (**13**) (1 g), 1-ethynyl-4-*t*butyl benzene , DMF(16mL), Pd(pph₃)₄(84mg), CuI (16 mg), triethylamine (37mL) were stirred in a RBF. A septum was secured on the flask with copper wire, and the reaction was heated at 100°C for 4h. Dichloromethane (100 mL) was added and the organic layer was washed with water (3 x 200 mL), brine, and the solvent was removed under reduced pressure. The solid was purified by column chromatography (DCM/hexanes 1:1) to yield 1.14 g (84%) of a bright orange solid. ¹H NMR (400MHz CDCl₃) δ 1.4 (9H, s), 7.51 (2H, d, *J* = 8.6 Hz), 7.65 (4H, m), 7.73 (2H, d, *J* = 8.6 Hz), 8.71 (2H, d, *J* = 7.8 Hz) 8.91 (2H, d, *J* = 8.6 Hz), 11.45 (1H, s). MALDI-TOF-MS *m/z*: calcd for C₂₇H₂₂O 362 obsd. 362.

9-((4-(*tert*-Butyl)phenyl)ethynyl)-10-ethynylantracene(**15**). Dimethyl (1-diazo-2-oxopropyl)phosphonate (0.7mL) was added dropwise under an inert atmosphere to a stirred 100mL round bottom flask containing **13** (1.5 g), anhydrous methanol (18mL), tetrahydrofuran (22 mL), and K₂CO₃ (1.136 g). A septum was secured to the flask using copper wire and the reaction was heated to 50 °C overnight. The reaction was checked using TLC and additional

Dimethyl (1-diazo-2-oxopropyl)phosphonate (0.2 mL) was added via syringe. After two days another TLC was taken, and the reaction had gone to completion, saturated NaHCO₃ (25 mL) and dichloromethane (50 mL) was added. The organic layer was washed with water (25 mL), brine (25 mL) dried (NaSO₄) and the solvent removed under reduced pressure. The solid was purified by column chromatography hexanes/DCM (95/5) to yield a yellow highly fluorescent solid. ¹H NMR (400MHz CDCl₃) δ 1.39 (9H, s), 4.08 (1H, s), 7.5 (2H, d, *J* = 8.6 Hz), 7.64 (4H, m), 7.72 (2H, d, *J* = 8.6Hz), 8.63 (2H, m), 8.7 (2H, m). MALDI-TOF-MS *m/z*: calcd for C₂₈H₂₂ 358 obsd. 358

BPEA 16. Toluene (30 mL) and quinuclidine (114 mg, 1.025 mmol) were bubbled with argon in a stirred round bottom flask at 0°C for 10 minutes. Allyl palladium(II) chloride dimer (19 mg, 5.2x10⁻² mmol), P(*t*-Bu)₃ (0.24 mL 1M in toluene), **12** (140 mg, 0.440 mmol), and **7**(262 mg, 0.440 mmol) were added in 5 minute increments while bubbling the solution with argon at 0°C. The flask was secured with a septum and copper wire, stirred at 60°C for 44 hours, cooled to room temp, and the solvent was removed under reduced pressure. The product was purified by column chromatography (93/7 DCM/MeOH) to yield 103.5mg (65%) of a bright yellow solid. ¹H NMR (400MHz CDCl₃) δ 1.38 (9H, s), 1.86 (7H, m), 2.07 (4H, m), 2.21 (1H, d, *J* = 14.1Hz), 2.54, (1H, m), 2.55 (3H, s), 2.92 (1H, m), 4.40 (1H, m), 7.36 (2H, d, *J* = 8.6Hz), 7.48 (2H, d, *J* = 8.6Hz), 7.64 (4H, m), 7.73 (4H, dd, *J* = 11.5, 8.4), 8.68 (4H, m) MALDI-TOF-MS *m/z*: calcd for C₄₅H₄₁N 595 obsd. 595

BPEA 17. BPEA **16**(100 mg, 0.168 mmol), CHCl₃ (2 mL), and CH₃I (2 mL) were place in a stirred round bottom flask under an argon atomosphere. The mixture was refluxed for 27 hours, filtered, and the solvent removed under reduced pressure to yield 108mg of a brown powder that was used without further purification.

Dyad 18. Dichloromethane (6 mL) and BPEA **17** (100 mg, 0.136 mmol) were placed in a stirred round bottom flask under a argon atomosphere at 0°C for 5 minutes. Triethylamine (100 µL) was added and the solution was stirred for 30 minutes. 6-Nitroso-1,10-phenanthroline-5-ol

(60mg, 0.266mmol) and 4Å (0.3 g) were added, then the reaction was refluxed overnight. Dichloromethane (90 mL) was added to the mixture, then washed with saturated NaHCO₃ (4 x 35 mL), water (2 x 35 mL), brine (2 x 35 mL), dried (Na₂SO₄), and the solvent was removed under reduced pressure. The product was purified by column chromatography (THF/NH₄OH 98/2) to yield 60.4 mg (57%) of a purple solid. ¹H NMR (400MHz CDCl₃) δ (ppm) 10.01 (1H, s), 9.07 (1H,m), 8.79 (2H, d, *J* = 6.3Hz), 8.7 (5H, m), 7.76 (2H, d, *J* = 8.2Hz), 7.72 (2H, d, *J* = 8.2Hz), 7.64 (5H, m), 7.53 (1H, m), 7.47 (4H, dd, *J* = 13.2, 8Hz), 7.42 (1H, m), 5.36 (1H, m), 3.94 (2H, m), 3.61 (3H, s), 2.6 (1H, d, *J* = 3.5Hz), 2.52 (1H, br. s), 2.27 (1H, d, *J* = 12.5Hz), 2.17 (5H, m), 2.05 (5H, m), 1.86 (3H, m), 1.38 (9H, s). MALDI-TOF-MS *m/z*: calcd for C₅₈H₄₈N₄O 816 obsd. 817.

BPEA 19. THF (1 mL) and triethylamine (1 mL) were bubbled with argon in a stirred round bottom flask at 0°C for 10 minutes. Tris(dibenzylideneacetone)dipalladium(0) (18 mg) and triphenylarsine (27 mg) were added and stirred for 10 minutes under an argon atmosphere. 4-Iodotoluene (30 mg, 0.14 mmol) was added and the mixture was stirred for an additional 5 minutes, with the subsequent addition of (30 mg, 0.14 mmol). The reaction mixture was stirred at room temperature overnight, and the solvent was removed under reduced pressure. The product was purified by column chromatography (hexane/dichloromethane 95/5) to yield 53.6 mg (86%) a bright yellow powder. ¹H NMR (400MHz CDCl₃) δ (ppm) 8.7 (4H, m), 7.7 (4H, m), 7.63(4H,m), 7.49 (2H, d, *J* = 8.2Hz), 2.44) 2.44 (3H, s), 1.38 (9H, s).

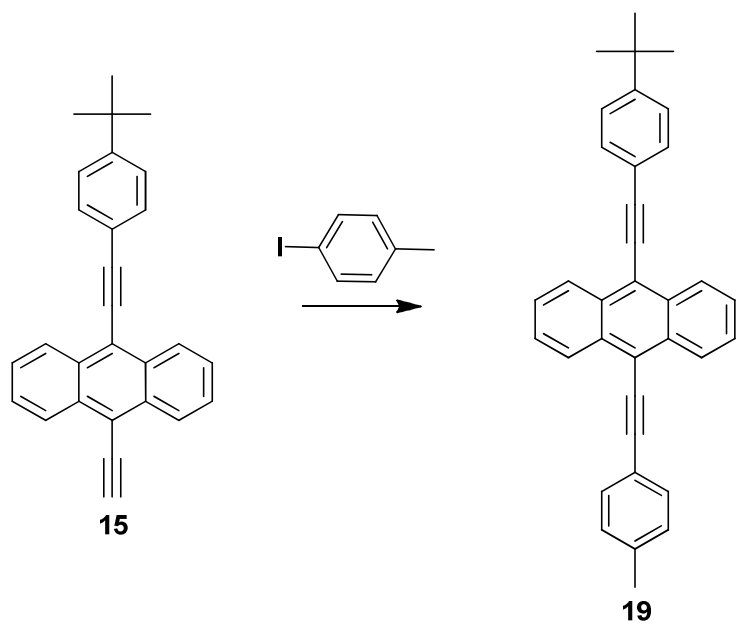


Figure 19. Synthetic scheme of Model 19

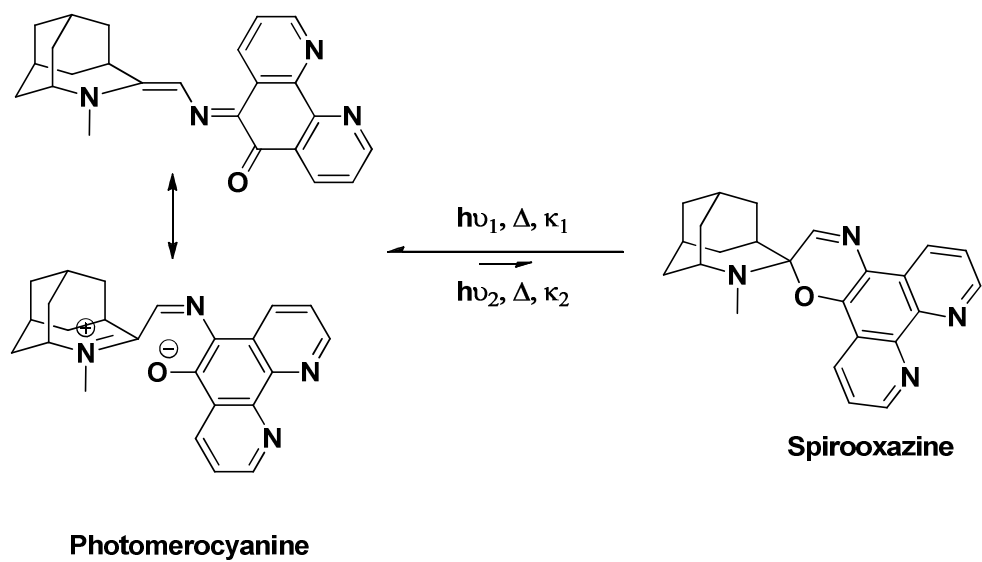


Figure 20. Photoisomerization of model photochrome

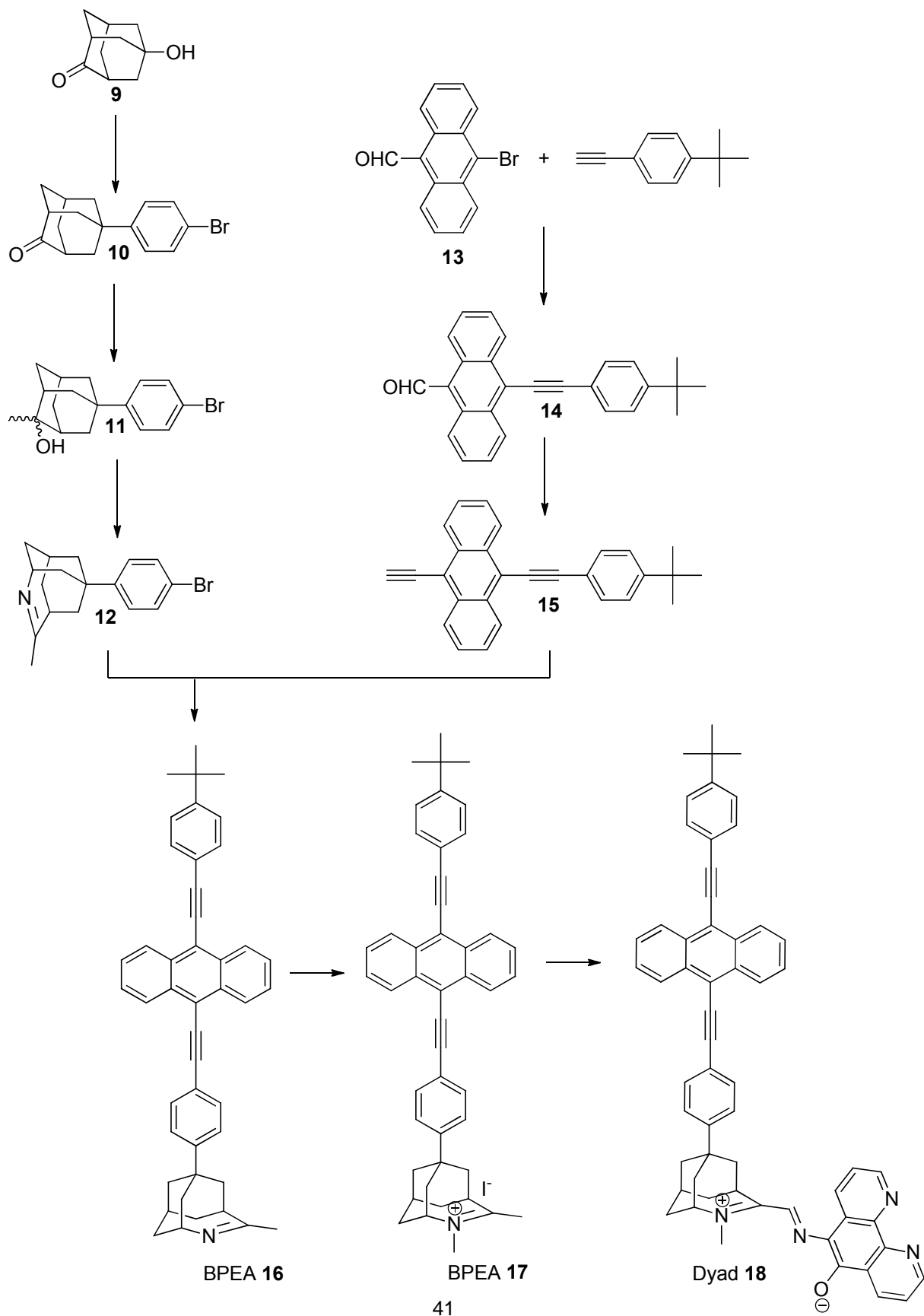
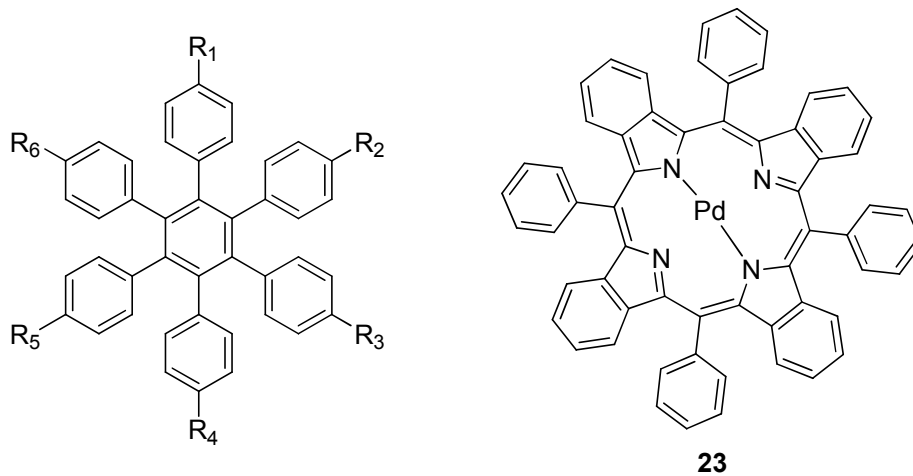


Figure 21. Synthetic scheme of Dyad 18

Experimental for Chapter 4. Triplet initiation was done by excitation of 20 by a 631.8nm He-Ne Metrologic Instruments laser. Using previously described methods hexa(4-iododphenyl)benzene(**19**)³², (4-bromophenyl)pentaphenylbenzene (**20**)³³ and *meso*-tetraphenyl-tetrabenzoporphyrin palladium (**23**)^{31,34} were synthesized.

Hexad 21. A solution of THF (2 mL) and triethylamine (2 mL) was bubbled with argon for 20 minutes. Then **19** (24.5 mg, 0.019 mmol), **15** (40.87 mg, 0.114 mmol), triphenylarsine (7 mg (0.023 mmol), and tris(dibenzylideneacetone)dipalladium(0) (3 mg, 0.0033 mmol) were added. The reaction was stirred overnight and the solvent was removed under reduced pressure. The product was purified by column chromatography hexane/dichloromethane 95/5) to yield 30.4mg (60%) of a bright yellow compound. ¹H NMR (400MHz CDCl₃) δ (ppm) 8.62 (m, 24H), 7.67 (d, 12H, *J* = 8.2 Hz), 7.51 (m, 36H), 7.45 (d, 12H, *J* = 8.6 Hz), 7.12 (d, 12H, *J* = 8.2 Hz), 1.36 (s, 54H). MALDI-TOF-MS *m/z* = calculated for C₁₁₀H₁₅₀ 2673.44, obsd. 2673.18.

Monomer 22. Toluene (30mL) and quinuclidine (57mg, 0.513mmol) were bubbled with argon in a stirred round bottom flask at 0°C for 20 minutes. Allyl palladium(II) chloride dimer (9.5 mg, 2.6x10⁻² mmol), P(*t*-Bu)₃ (0.12 mL 1M in toluene), **20** (134.98 mg, 0.220 mmol), and **15** (78.9 mg, 0.220 mmol) were added in 5 minute intervals while bubbling the solution with argon at 0°C. The flask was secured with a septum and copper wire, stirred at 60°C for 24 hours, cooled to room temp, and the solvent was removed under reduced pressure. The product was purified by column chromatography (hexane dichloromethane 97/3) to yield 140mg (0.158 mmol) of a bright yellow powder. ¹H NMR (400MHz CDCl₃) δ (ppm) 8.66 (m, 2H), 8.59 (m, 2H), 7.7 (d, 2H, *J* = 8.2 Hz), 7.59 (m, 4H), 7.48 (d, 2H, *J* = 8.6 Hz), 6.89, (m, 27H), 1.38 (s, 9H). MALDI-TOF-MS *m/z* = calculated for C₇₀H₅₀ 891.15, obsd. 891.28



19: R₁ = R₂ = R₃ = R₄ = R₅ = R₆ = I

20: R₁ = R₂ = R₃ = R₄ = R₅ = H, R₆ = Br

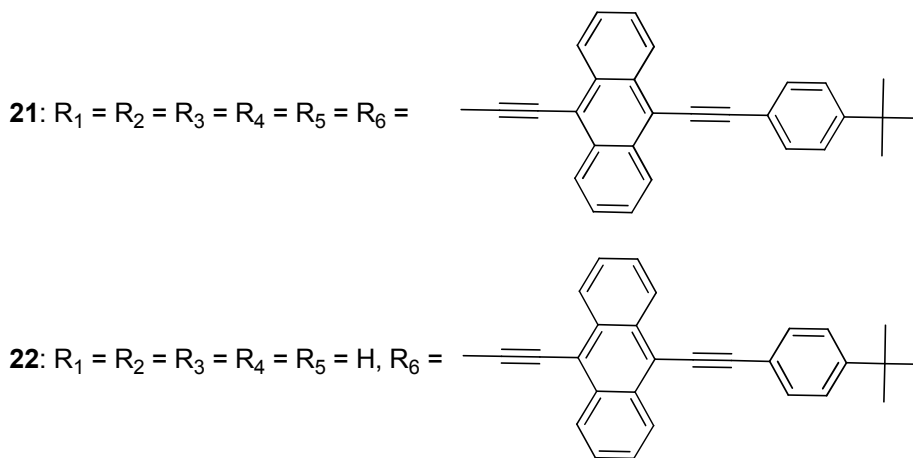


Figure 22: Synthetic intermediates and final compounds required for TTA-UC

REFERENCES

- (1) Douglas A. Skoog; F. James Holler; Nieman, T. A.: *Principles of Instrumental Analysis*; Fifth ed.; Thompson Learning: United States of America, 1998. pp. 356-353.
- (2) Marcus, R. A. *Journal of Chemical Physics* **1956**, *24*, 966-978.
- (3) Levich, V. G. *Advances in Electrochemistry and Electrochemical Engineering* **1946**, *5*, 249-371.
- (4) Förrester, T. *Annals of Physics* **1948**, *2*, 1948.
- (5) Förrester, T. *Naturwissenschaften* **1946**, *33*, 165-175.
- (6) Masahiro, I. *Chemical Reviews* **2000**, *100*, 1685-1716.
- (7) John C. Crano; Gugliemetti, R.: *Photochromic and Thermochromic Compounds*; Plenum Press: New York, 1999; Vol. 1.
- (8) Berkvoic, G.; Krongauz, V.; Wiess, V. *Chemical Reviews* **2000**, *100*, 1741-1754.
- (9) Parker, C. A.; Hatchard, C. G. *Proc. Chem. Soc. London* **1962**.
- (10) Parker, C. A. *Chemical Communications* **1964**, 749-750.
- (11) Keivanidis, P. E.; Balushev, S.; Miteva T.; Nelles, G.; Scherf, U.; Yasunda, A.; Wegner, G. *Advance Materials* **2005**, *15*, 2095.
- (12) Islangulov, R. R.; Koslov, D. V.; Castellano, F. N. *Journal of the American Chemical Society* **2007**, *129*, 12652-12653.
- (13) Trupke, T.; Shalava, A.; Richards, B. S.; Würfel, P.; Green, M. A.: In *Solar Energy Materials Solar Cells*, 2006; Vol. 90; pp 3327-3328.
- (14) Walz, J.; Ulrich, K.; Port, H.; Wolf, H. C.; Wonner, J.; Effenberger, F. *Chemical Physics Letters* **1993**, *213*, 321-324.
- (15) Fernandez-Acebes, A.; Lehn, J. M. *Chemistry-A European Journal* **1999**, *5*, 3285-3292.
- (16) Norsten, T. B.; Branda, N. R. *Journal of the American Chemical Society* **2001**, *123*, 1784-1785.
- (17) Mitchell, R. H.; Ward, T. R.; Chen, Y.; Weerawanna S. A.; Dibble, P. W.; Marella, M. J.; Almutairi, A.; Wang, Z. *Journal of the American Chemical Society* **2003**, *125*, 2974-2988.
- (18) Liddell, P. A.; Kodis, G.; Moore, A. L.; Moore, T. A.; Gust*, D. *Journal of the American Chemical Society*. **2002**, *124*, 7668-7669.
- (19) Endtner, J. M.; Effenberger, F.; Hartschuh, A.; Port, H. *Journal of the American Chemical Society*. **2000**, *122*, 3037-3046.

- (20) Hanazawa, M.; Sumiya, R.; Horikawa, Y.; Irie, M. *Chemical Communications*. **1992**, 206.
- (21) Lucas, L. N.; Esch, J. v.; Kellogg, R. M.; Feringa, B. L. **1998**, 2313–2231.
- (22) Peters, A.; Branda, N. R.. *Advanced Materials for Optics and Electronics*. **2000**, 10, 245-249.
- (23) Straight, S. D.; Kodis, G.; Terazono, Y.; Hambourger, M.; Moore, T. A.; Moore, A. L.; Gust, D. *Nature Nanotechnology*. **2008**, 3, 280-283.
- (24) Raymo, F.; Tomasulo, M. *Chemical Society Reviews* **2005**, 34, 327-336.
- (25) Keirstead, A. E.; Bridgewater, J. W.; Terazono, Y.; Kodis, G.; Straight, S.; Liddell, P. A.; Moore, A. L.; Moore, T. A.; Gust, D. *Journal of the American Chemical Society* **2010**, 132, 5688-6595.
- (26) Patel, D. G.; Paquette, M. M.; Kopelman, R. A.; Kaminsky, W.; Ferguson M. J.; Frank, N. L. *Journal of the American Chemical Society* **2010**, 132, 12568-12586.
- (27) Lewis, N. S.; Nocera, D. G. *Proceedings of the National Academy Science*. **2006**, 103, 15729-15735.
- (28) *International Energy Outlook*; Energy, U. S. D. o., 2007.
- (29) Kamat, P. V. *Journal of Physical Chemistry, C* **2007**, 111, 1834-2860.
- (30) Luque, A.; S., H.: *Handbook of Photovoltaic Science and Engineering*; John Wiley and Sons: Hoboken, NJ, 2003.
- (31) Koprnenkov, V. N.; Dashkevich, S. N.; Lukyanets, E. A. *Zhurnal Obshchei Khimii* **1981**, 51, 2513-2517.
- (32) Kobayashi, K.; Kobayashi, N.; Ikuta, M.; Therrien, B.; Sakamoto, S.; Yamaguchi, K. *Journal of Organic Chemistry* **2005**, 70, 749-752.
- (33) Kübel, C.; Chen, S.-L.; Müllen, K. *Macromolecules* **1998**, 31, 6014-6021.
- (34) Perez, D. M.; Borek, C.; Forrest, S.; Thompson, M. *Journal of the American Chemical Society* **2009**, 9281-9286.

This document was generated using the Graduate Education Format Advising tool. Please turn a copy of this page in when you submit your document to Graduate College format advising. You may discard this page once you have printed your final document. **DO NOT TURN THIS PAGE IN WITH YOUR FINAL DOCUMENT!**

Font Type: Arial

Font size: 10